RHIC Beam Energy Scan Program: an Update

Michal Šumbera
Nuclear Physics Institute AS CR, Řež/Prague
(for the STAR Collaboration)

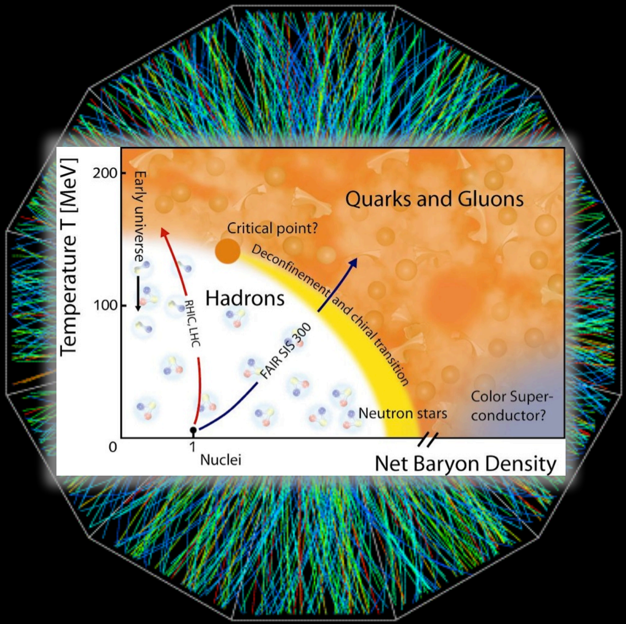

ZIMÁNYI SCHOOL'17 **Dec. 4. - Dec. 8., Budapest, Hungary**

The RHIC Beam Energy Scan Motivation

1) Turn-off of sQGP signatures

2) Search for the signals of phase boundary

3) Search for the QCD critical point

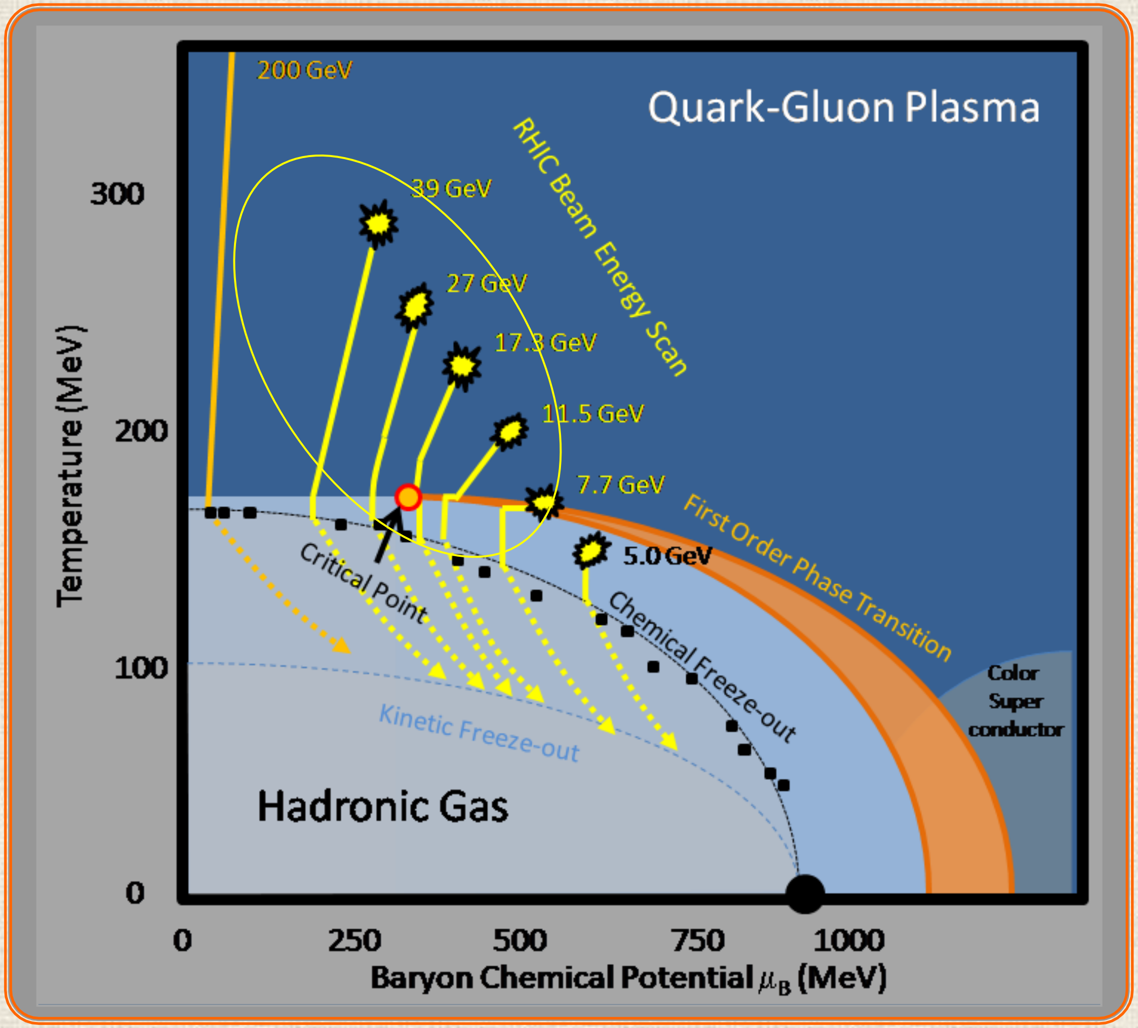

http://arxiv.org/abs/1007.2613

The QCD Phase Diagram and BES

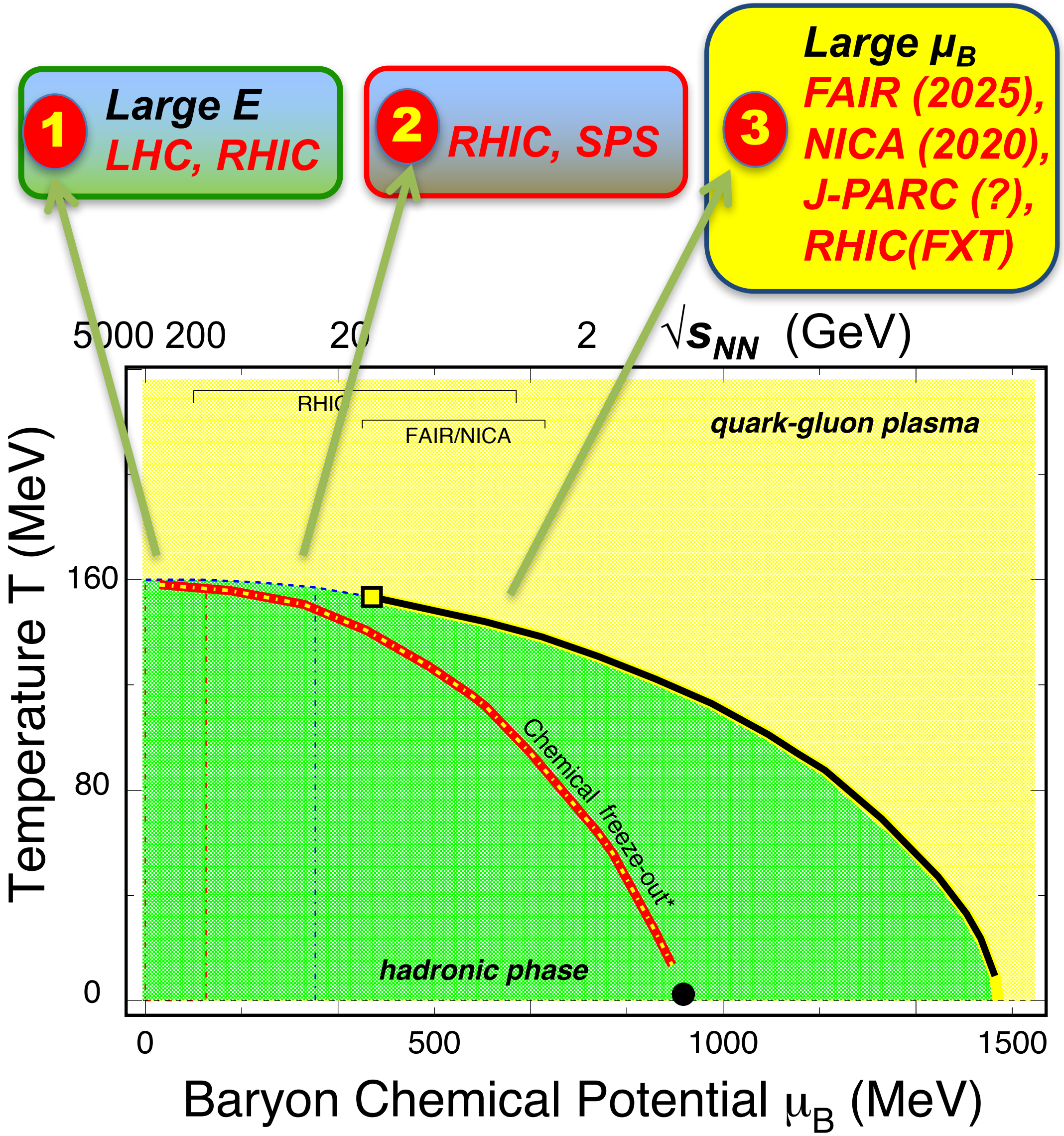

2000–2012: RHIC+LHC

Top energy program

Discovery of sQGP

- QCD **Critical Point?**
- Chiral effects**?**

2010–2017: RHIC BES-I

7.7, 11.5, 14.5, 19.6, 27, 39, 54.4 GeV

2019–2020: RHIC BES-II

7.7, 11.5, 9.1, 14.5, 19.6 GeV

FXT*: 3.0, 3.5, 3.9, 4.5, 7.7 GeV

2022 – : RHIC+FAIR BES-III

Fixed-target programs

The STAR Detector System

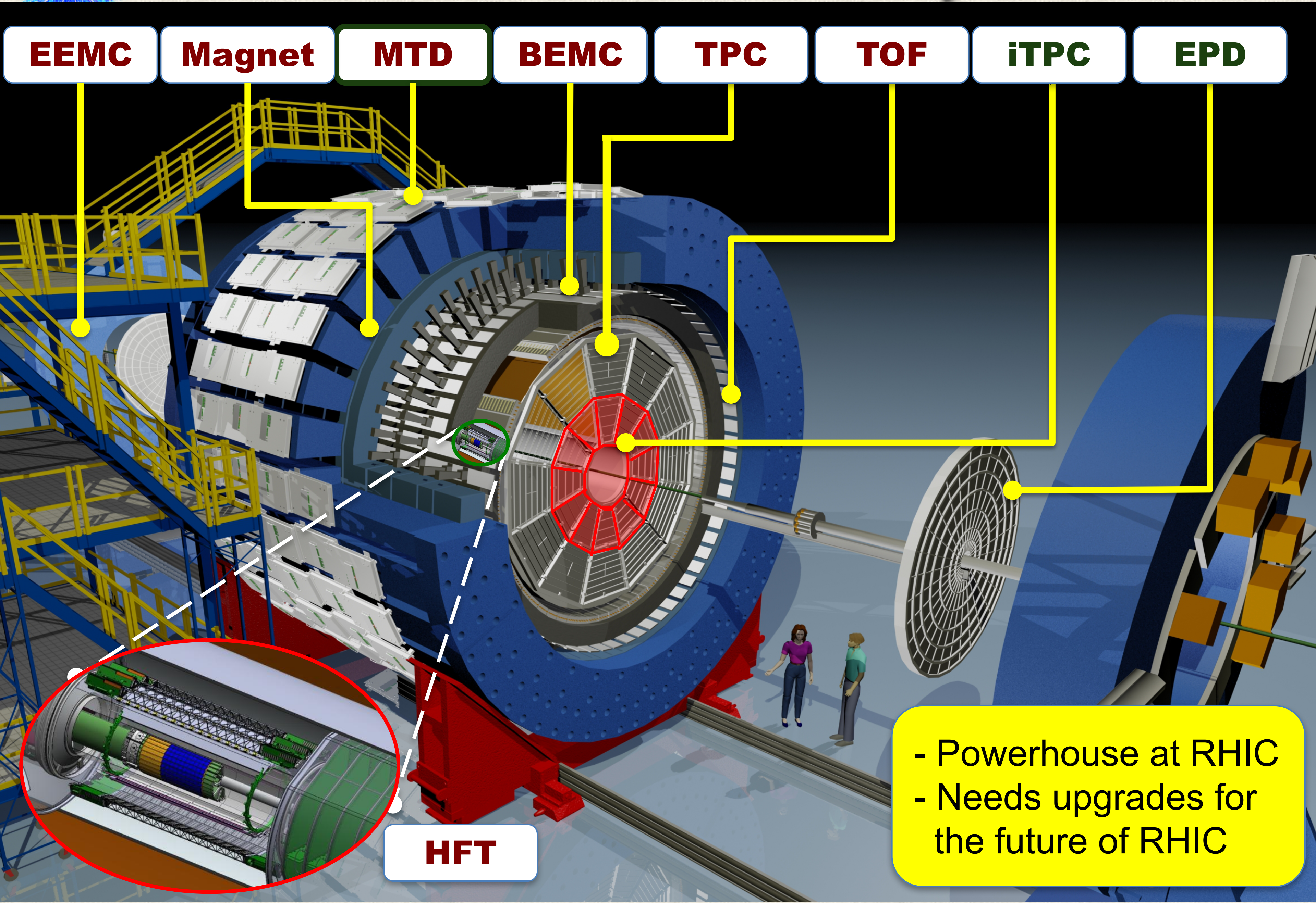

- Powerhouse at RHIC
- Needs upgrades for the future of RHIC

BES-I Au+Au Data Taking

Largest data sets versus collision energy!!!

$\sqrt{s_{NN}}$ [GeV]	events(10^6)	Year
200	350	2010
62.4	67	2010
54.4	300	2017
39	130	2010
27	70	2011
19.6	36	2011
14.5	20	2014
11.5	12	2010
7.7	5	2010
4.9 (FXT)	3.4	2015
4.5 (FXT)	1.3	2015

Geometric acceptance @ collider mode remains the same, track density gets lower.
Detector performance generally improves at lower energies.

STAR: Phys.Rev. C **96** (2017) 044904

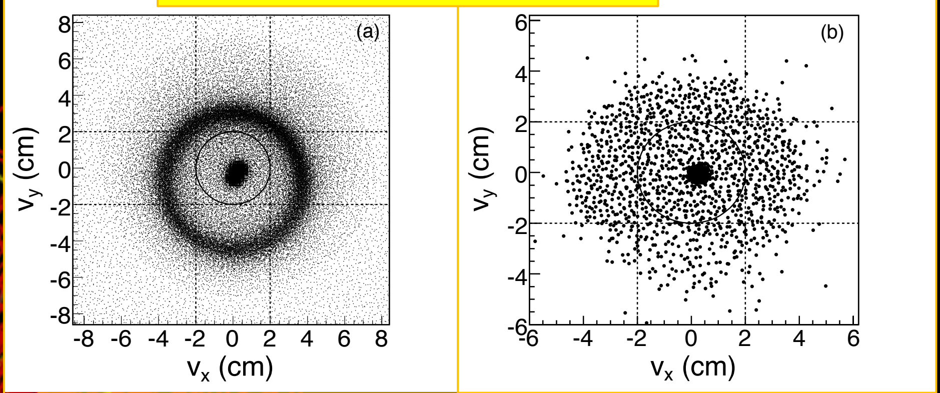

x and y distribution of reconstructed vertex at $\sqrt{s_{NN}}$=7.7 GeV (a) and $\sqrt{s_{NN}}$=39 GeV (b)

STAR: Phys.Rev. C **96** (2017) 044904

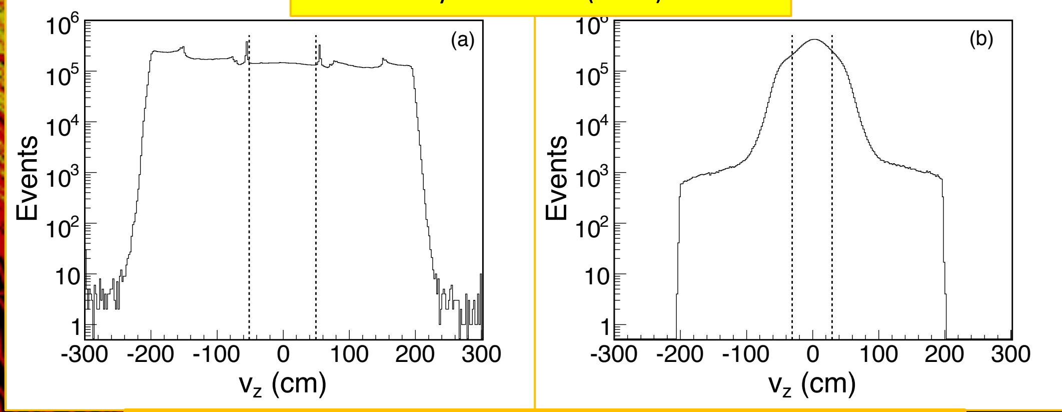

z distribution of reconstructed vertex at $\sqrt{s_{NN}}$=7.7 GeV (a) and $\sqrt{s_{NN}}$=39 GeV (b)

BES-I Au+Au Data Taking

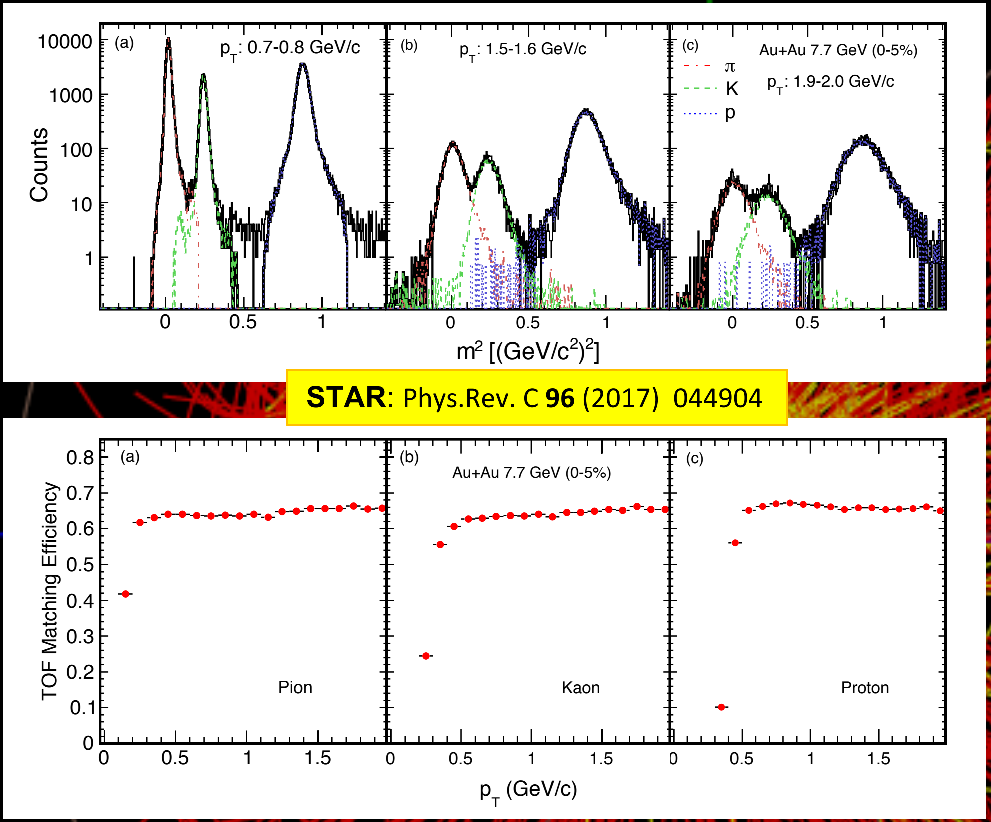

STAR: Phys.Rev. C **96** (2017) 044904

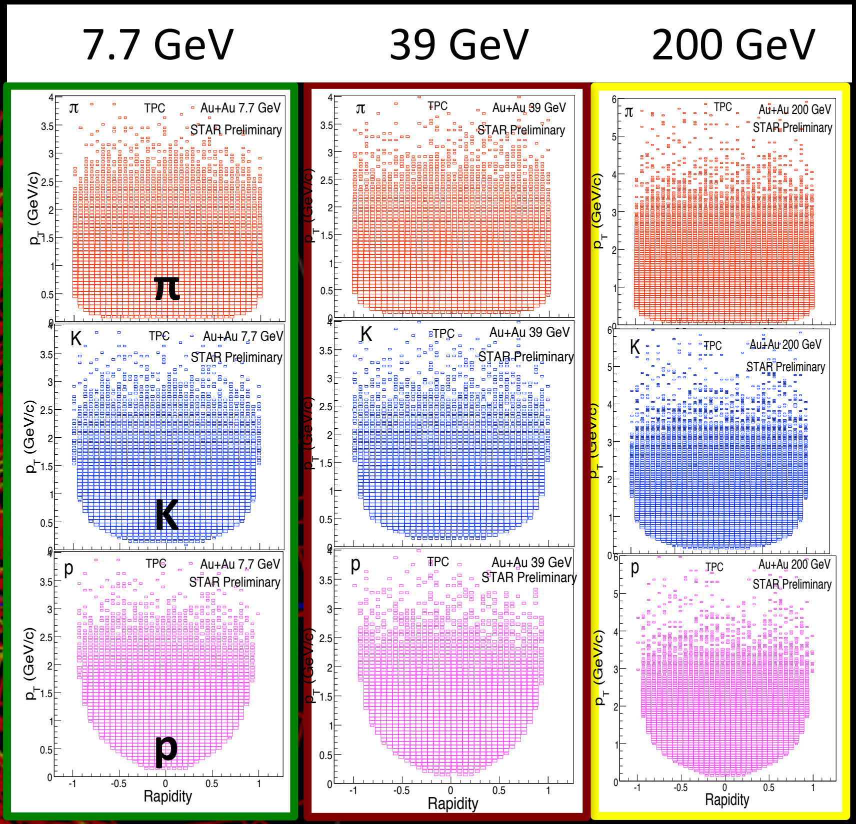

Excellent particle identification capabilities. Large and homogeneous acceptance.
Especially important for fluctuation analysis

Hadron Spectra from BES-I

$\sqrt{s_{NN}}$ = *19.6* GeV Au+Au Collisions

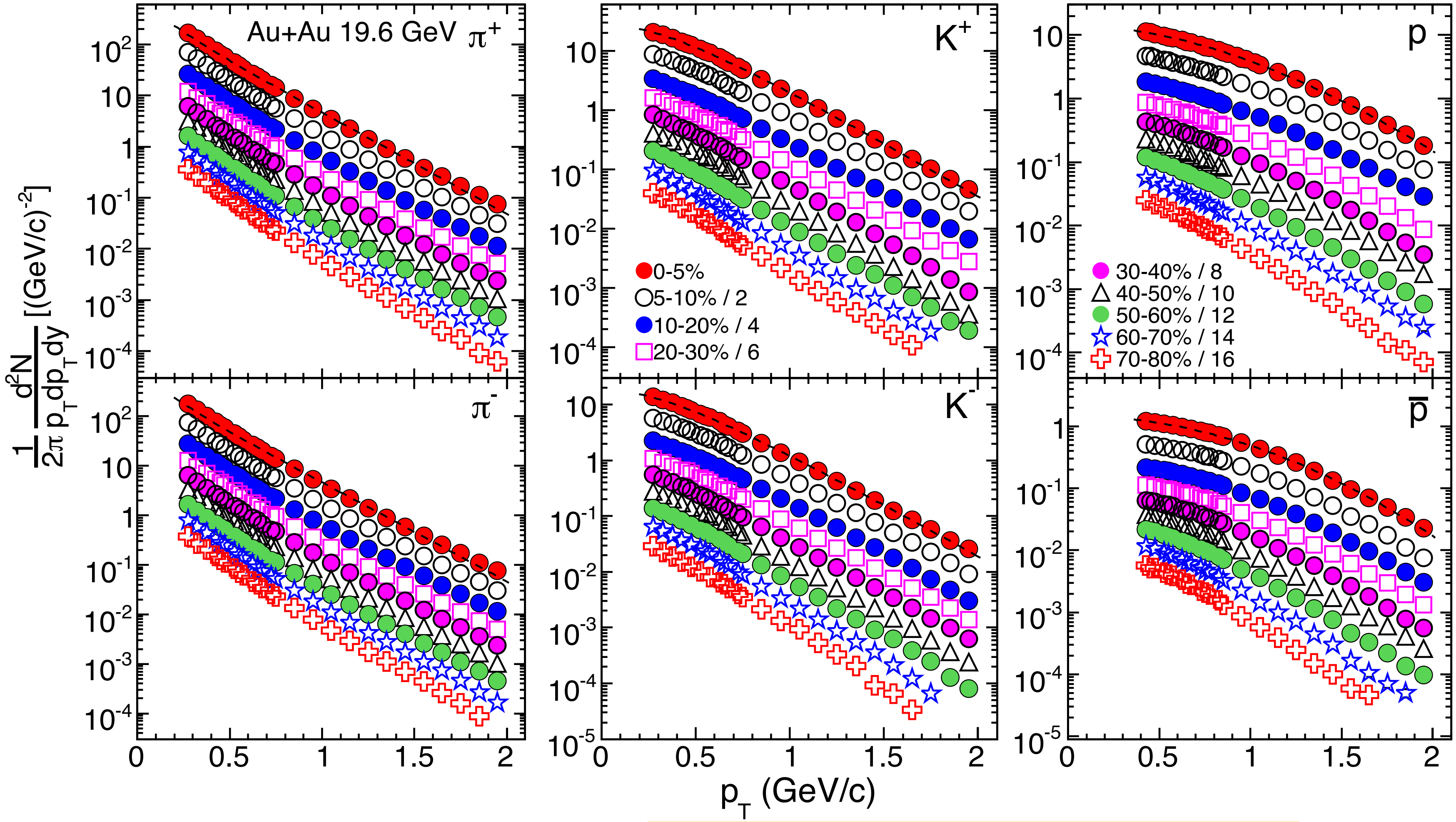

STAR: Phys.Rev. C **96** (2017) 044904

Hadron Spectra from BES-I

$\sqrt{s_{NN}}$ = 27 GeV Au+Au Collisions

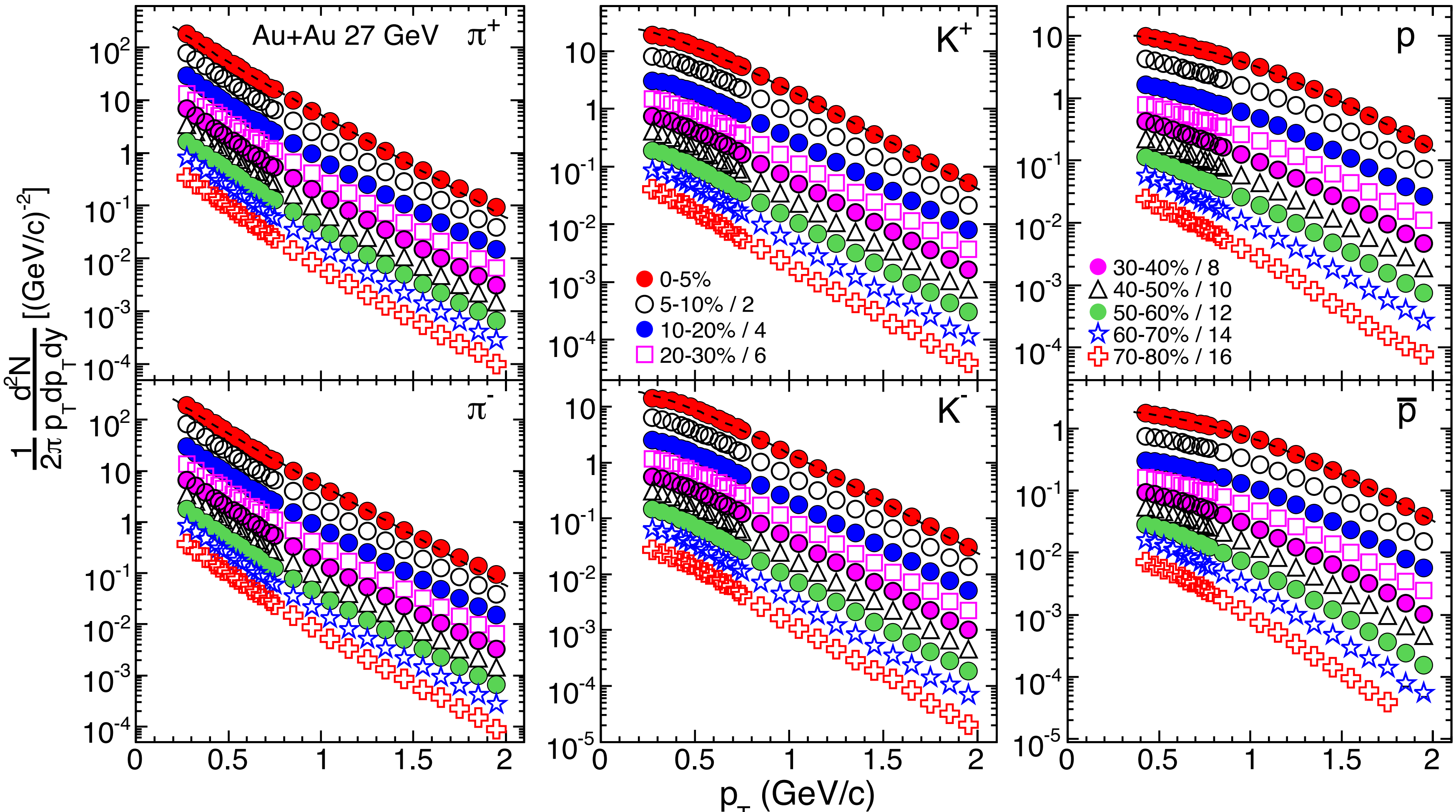

STAR: Phys.Rev. C **96** (2017) 044904

STAR publications on BES results

1. Inclusive charged hadron elliptic flow in Au + Au collisions at $\sqrt{s_{NN}}$= 7.7-62.4 GeV , Phys. Rev. **C 86** (2012) 54908
2. Observation of an energy-dependent difference in elliptic flow between particles and antiparticles in relativistic heavy ion collisions, Phys. Rev. Lett. **110** (2013) 142301
3. Elliptic flow of identified hadrons in Au+Au collisions at $\sqrt{s_{NN}}$= 7.7-62.4 GeV , Phys. Rev. C **88** (2013) 14902

at the time of my last talk at this conference in 2013

STAR publications on BES results

1. Inclusive charged hadron elliptic flow in Au + Au collisions at $\sqrt{s_{NN}}$= 7.7-62.4 GeV , Phys. Rev. **C 86** (2012) 54908
2. Observation of an energy-dependent difference in elliptic flow between particles and antiparticles in relativistic heavy ion collisions, Phys. Rev. Lett. **110** (2013) 142301
3. Elliptic flow of identified hadrons in Au+Au collisions at $\sqrt{s_{NN}}$= 7.7-62.4 GeV , Phys. Rev. C **88** (2013) 14902
4. Energy Dependence of Moments of Net-proton Multiplicity Distributions at RHIC , Phys.Rev.Lett. **112** (2014) 032302
5. Beam-Energy Dependence of the Directed Flow of Protons, Antiprotons, and Pions in Au+Au Collisions , Phys.Rev.Lett. **112** (2014) 162301
6. Beam energy dependence of moments of the net-charge multiplicity distributions in Au+Au collisions at RHIC , Phys.Rev.Lett. **113** (2014) 092301
7. Beam-energy-dependent two-pion interferometry and the freeze-out eccentricity of pions measured in heavy ion collisions at the STAR detector , Phys.Rev. C **92** (2015) 014904

STAR publications on BES results

8. Energy dependence of acceptance-corrected dielectron excess mass spectrum at mid-rapidity in Au+Au collisions at $\sqrt{s_{NN}}$= 19.6 and 200 GeV, Phys.Lett. B **750** (2017) 64
9. Beam-energy dependence of charge separation along the magnetic field in Au+Au collisions at RHIC , Phys.Rev.Lett. **113** (2014) 052302
10. Energy Dependence of K/π, p/π, and K/p Fluctuations in Au+Au Collisions from $\sqrt{s_{NN}}$ = 7.7 to 200 GeV , Phys.Rev. C **92** (2015) 021901
11. Observation of charge asymmetry dependence of pion elliptic flow and the possible chiral magnetic wave in heavy-ion collisions , Phys.Rev.Lett. **114** (2015) 252302
12. Probing parton dynamics of QCD matter with Ω and φ production, Phys.Rev. C **93** (2016) 021903
13. Beam-energy dependence of charge balance functions from Au + Au collisions at energies available at the BNL Relativistic Heavy Ion Collider , Phys.Rev. C **94** (2016) 024909
14. Centrality dependence of identified particle elliptic flow in relativistic heavy ion collisions at $\sqrt{s_{NN}}$=7.7–62.4 GeV , Phys.Rev. C **93** (2016) 014907
15. Beam Energy Dependence of the Third Harmonic of Azimuthal Correlations in Au+Au Collisions at RHIC , Phys.Rev.Lett. **116** (2016) 112302

STAR publications on BES results

16. Measurement of elliptic flow of light nuclei at $\sqrt{s_{NN}}$= 200, 62.4, 39, 27, 19.6, 11.5, and 7.7 GeV at the BNL Relativistic Heavy Ion Collider, Phys.Rev. C **94** (2016) 034908

17. Energy dependence of J/ψ production in Au+Au collisions at $\sqrt{s_{NN}}$= 39, 62.4 and 200 GeV, Phys.Lett. B **771** (2017) 13

18. Harmonic decomposition of three-particle azimuthal correlations at RHIC, arXiv:1701.06496

19. Global Λ hyperon polarization in nuclear collisions: evidence for the most vortical fluid, **Nature 548**, 62 (2017)

20. Bulk Properties of the Medium Produced in Relativistic Heavy-Ion Collisions from the Beam Energy Scan Program, Phys.Rev. C **96** (2017) 044904

21. Beam Energy Dependence of Jet-Quenching Effects in Au+Au Collisions at $\sqrt{s_{NN}}$ = 7.7, 11.5, 14.5, 19.6, 27, 39, and 62.4 GeV , arXiv:1707.01988

22. Beam-Energy Dependence of Directed Flow of Λ, antiΛ, $K^{\pm}$, K^0_s and φ in Au+Au Collisions , arXiv:1708.07132, accepted to Phys.Rev.Lett.

23. Collision Energy Dependence of Moments of Net-Kaon Multiplicity Distributions at RHIC, arXiv:1709.00773

+ many conference proceedings…

1. Turn-off of sQGP signatures

Suppression of Charged Hadrons and its Disappearance

STAR: arXiv:1707.01988

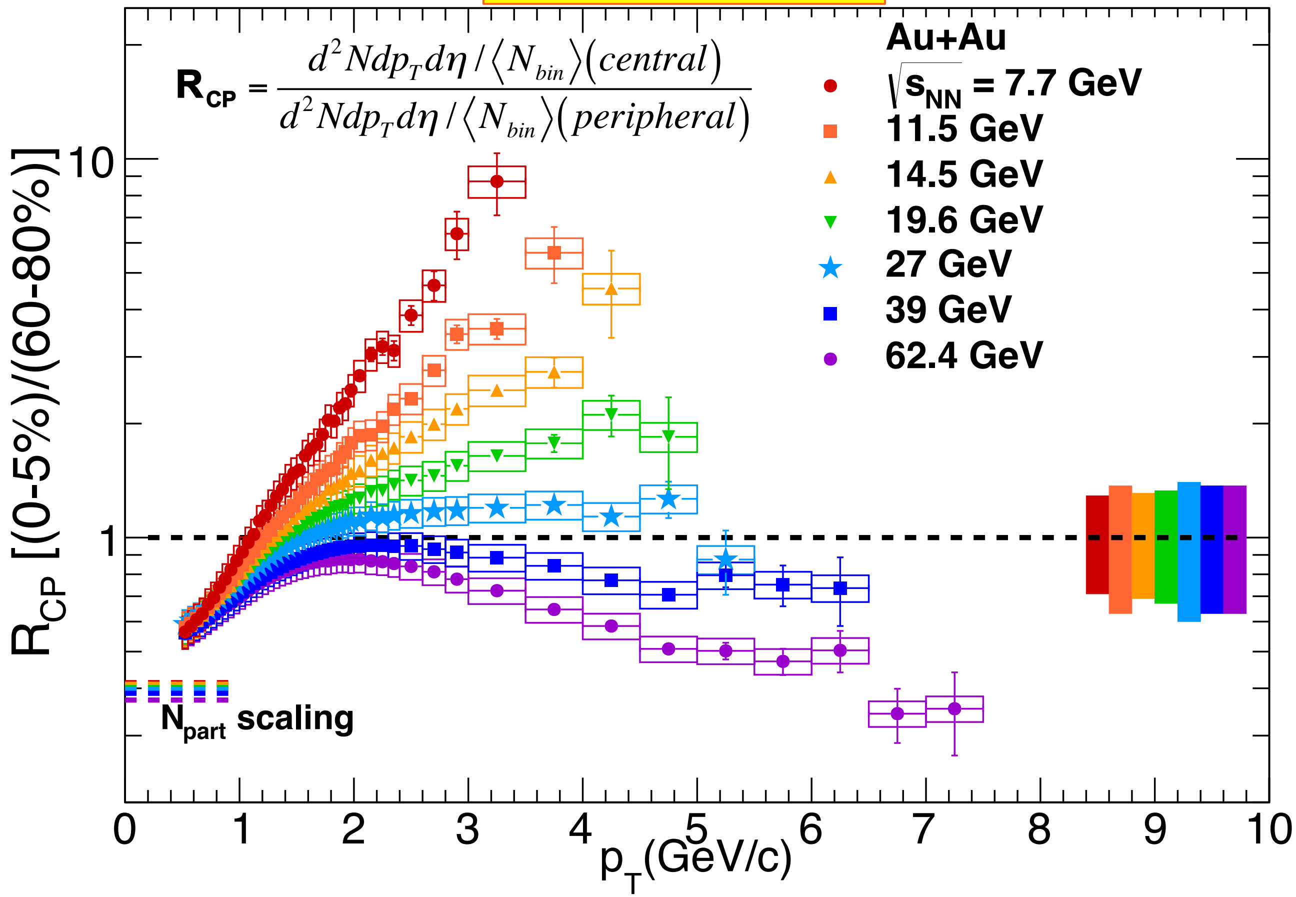

$$N_{bin}(b)=N_{coll}(b)=\sigma^{in}{}_{NN}T_{AB}(b)$$

$$T_{AB}(\mathbf{b}) \equiv \int d^2\mathbf{s}\; T_A(\mathbf{s})T_B(\mathbf{b}-\mathbf{s})$$

$$T_A(\mathbf{b}) \equiv \int dz\rho_A(z,\mathbf{s})$$

$$N_{part}(b)=$$

$$\int d^2\mathbf{s}\; T_A(\mathbf{s})\left(1-e^{-\sigma_{NN}^{in}T_B(\mathbf{s})}\right)$$

$$+$$

$$\int d^2\mathbf{s}\; T_B(\mathbf{s}-\mathbf{b})\left(1-e^{-\sigma_{NN}^{in}T_A(\mathbf{s})}\right)$$

R.P.+M.Š.: arXiv:1611.01533

$R_{CP} \geq 1$ at lower energies - Cronin effect?

Identified particles R_{CP}

STAR: arXiv:1707.01988

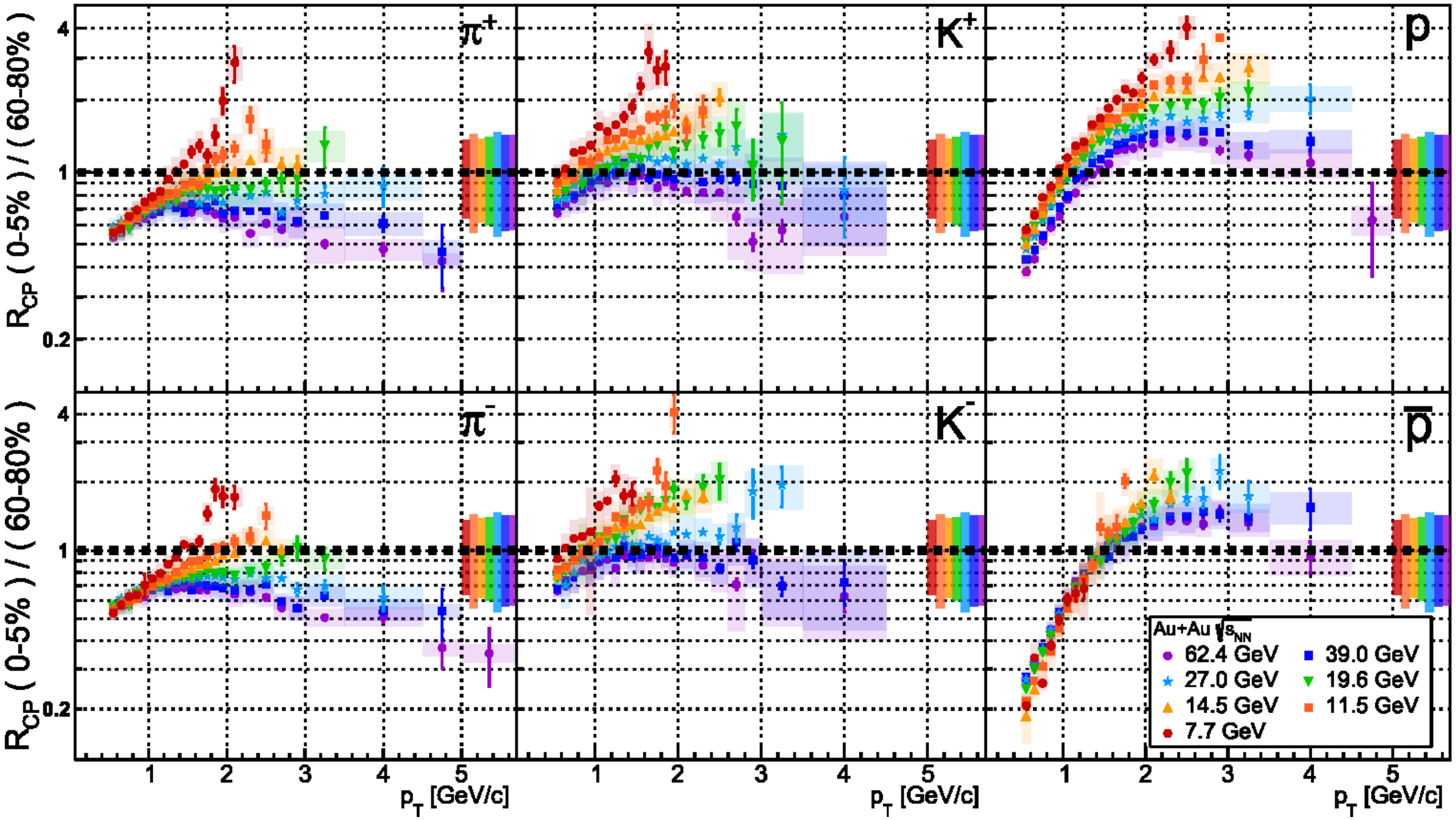

(Feed-down subtracted)

High-p_T suppression and its further evolution into enhancement at lower energies is driven by mesons. Baryons remain enhanced up to $\sqrt{s_{NN}}$=62.4 GeV
⇒ Mass driven phenomenon?

Binary collision scaled yield Y(<N_{part}>)

Take the numerator from R_{CP} and plot it versus centrality:

$$Y(\langle N_{\rm part}\rangle) = \frac{1}{\langle N_{\rm coll}\rangle}\frac{d^2N}{dp_{\rm T}d\eta}(\langle N_{\rm part}\rangle)$$

N.B. The peripheral bin contents are in the first bin at low <N_{part}> and the central bin's contents are in the last point at high <N_{part}>.

😊 Examining the full centrality evolution allows determine whether the processes leading to enhancement increase faster or slower than the processes leading toward suppression as a function of <N_{part}>.

⇒The non-monotonic shape results from the faster increase of jet-quenching compared to the combined phenomena leading to enhancement.*

STAR: arXiv:1707.01988

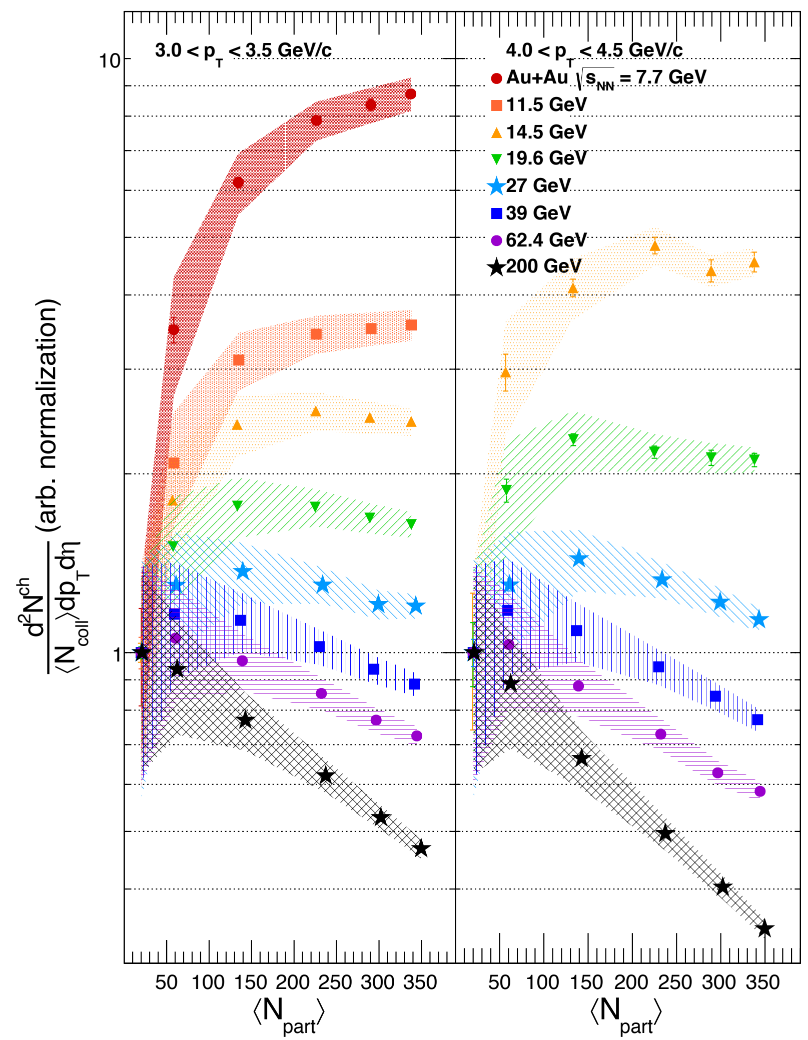

*)Does not rule out the possibility that QGP is also formed @ $\sqrt{s_{NN}}$ < 14.5 GeV

J/ψ Suppression at 39, 62.4 and 200 GeV

STAR: Phys.Lett. B771 (2017) 13-20

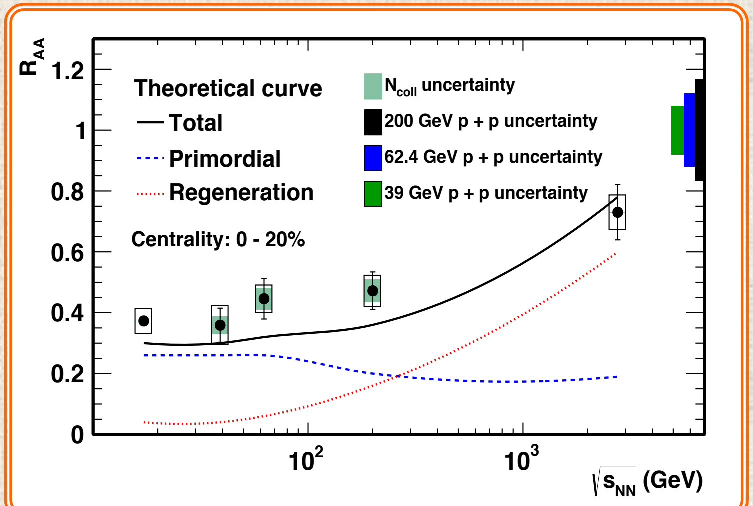

$$R_{AA} = \frac{\sigma_{inel}^{pp}}{< N_{coll} >} \frac{d^2N_{AA}/dpTdy}{d^2\sigma_{pp}/dpTdy}$$

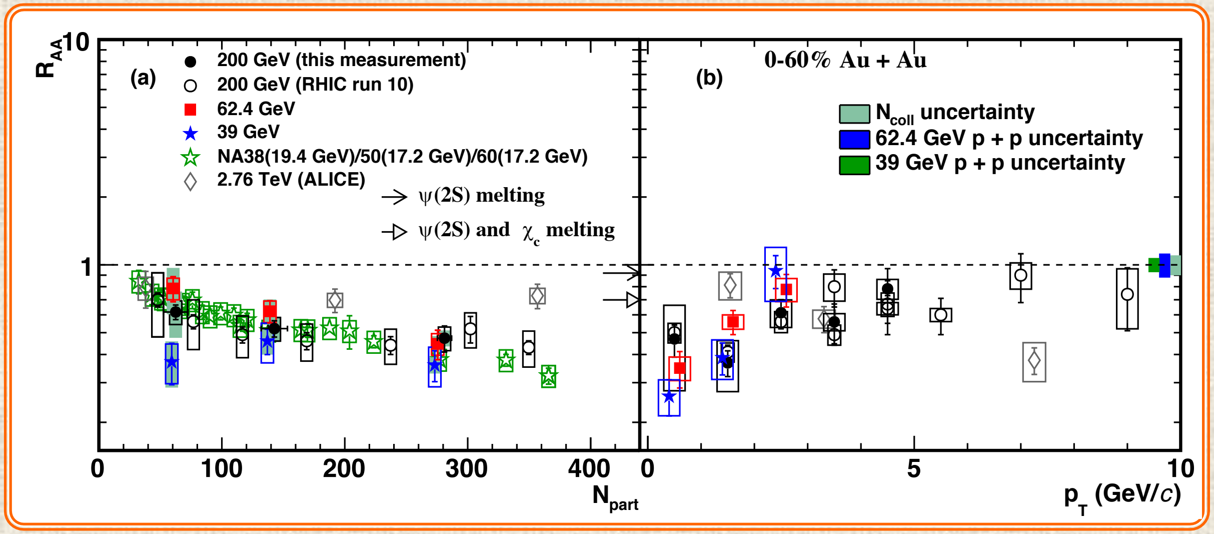

- ★ At all three energies R_{AA}<1.
- ★ Consistent* with the suppression of directly produced J/ψ mesons.
- ★ No significant energy dependence of R_{AA} is found within uncertainties.
- ★ Model calculations*, which include direct suppression and regeneration, describe reasonably well the (centrality and) energy dependence of J/ψ production.

NA38: M.C. Abreu et al., Phys. Lett. B 477, 28 (2000)
ALICE: B. Abelev et al., Phys. Lett. B 734, 314 (2014)

*) Model: X. Zhao and R. Rapp, Phys. Rev. C 82, 064905 (2010)

e^+e^- production at 27,39, 62.4 and 200 GeV

STAR: Phys.Lett. B750 (2015) 64-71

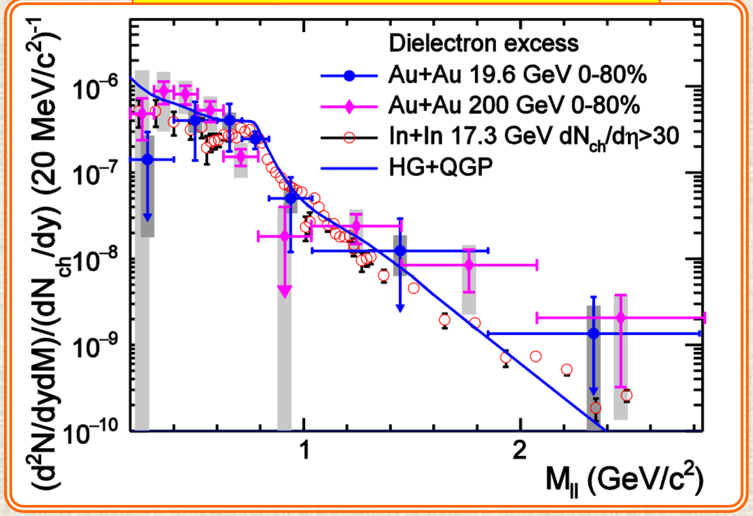

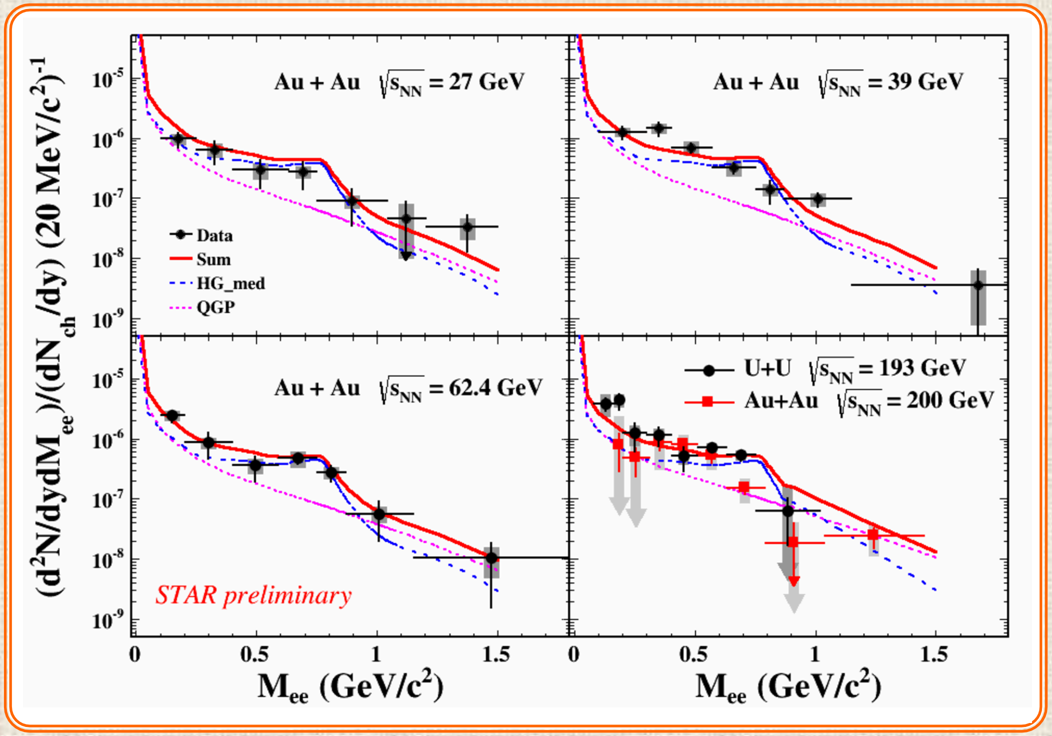

★ Acceptance-corrected excess mass spectra are well described by an effective many body calculations* that incorporate a broadened ρ spectral function in various collision systems and energies.

*) Theory:
R. Rapp, PRC 63 (2001) 054907
and private communication

☛ The QGP contribution is still significant in the LMR at the lowest energy.
⇒ The integrated yield can be used as a probe for the turn-off of the QGP in the future BES-II program at RHIC.

Connection to fireball lifetime

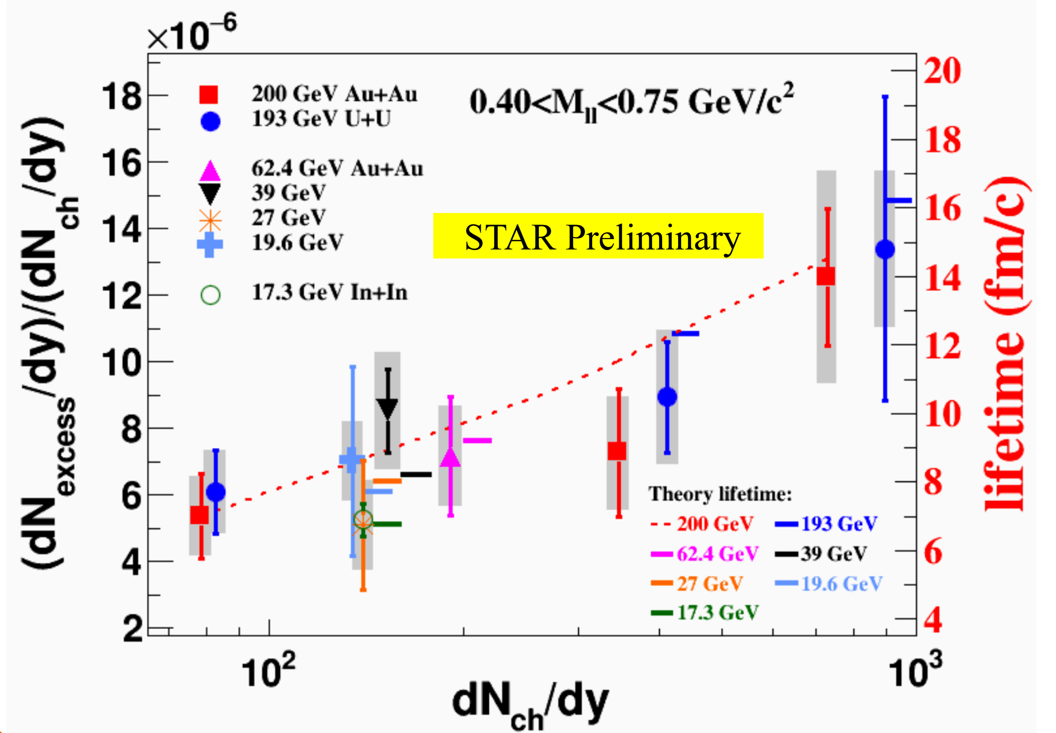

Theory:
R. Rapp, H. van Hees
PLB 753 (2016) 586-590

- ★ From $\sqrt{s_{NN}}$ = 17.3 GeV to $\sqrt{s_{NN}}$ = 200 GeV the integrated excess yield,normalized by dN_{ch}/dy, is proportional to lifetime of the fireball.
- ★ The fireball lifetime also increases linearly with the collision centrality (40-80%, 10-40%, 0-10%) is observed too.

2. Search for the signals of phase boundary: Azimuthal correlations

Directed Flow of Λ, $K^{\pm}$, K^0_s and φ

STAR: arXiv:1708.07132, PRL (accepted)

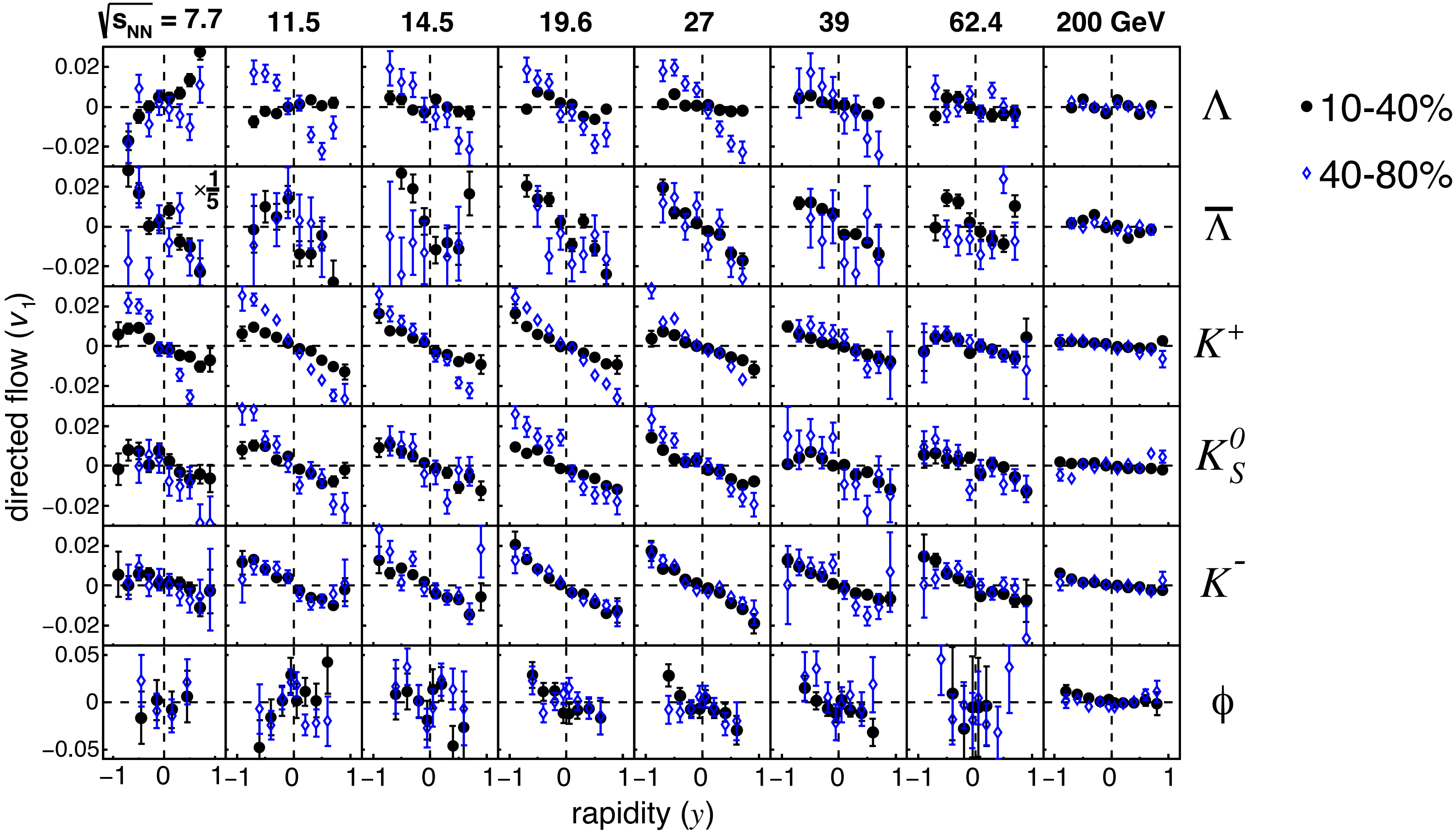

Directed Flow of Λ, $K^{\pm}$, K^0_s, φ and p, π

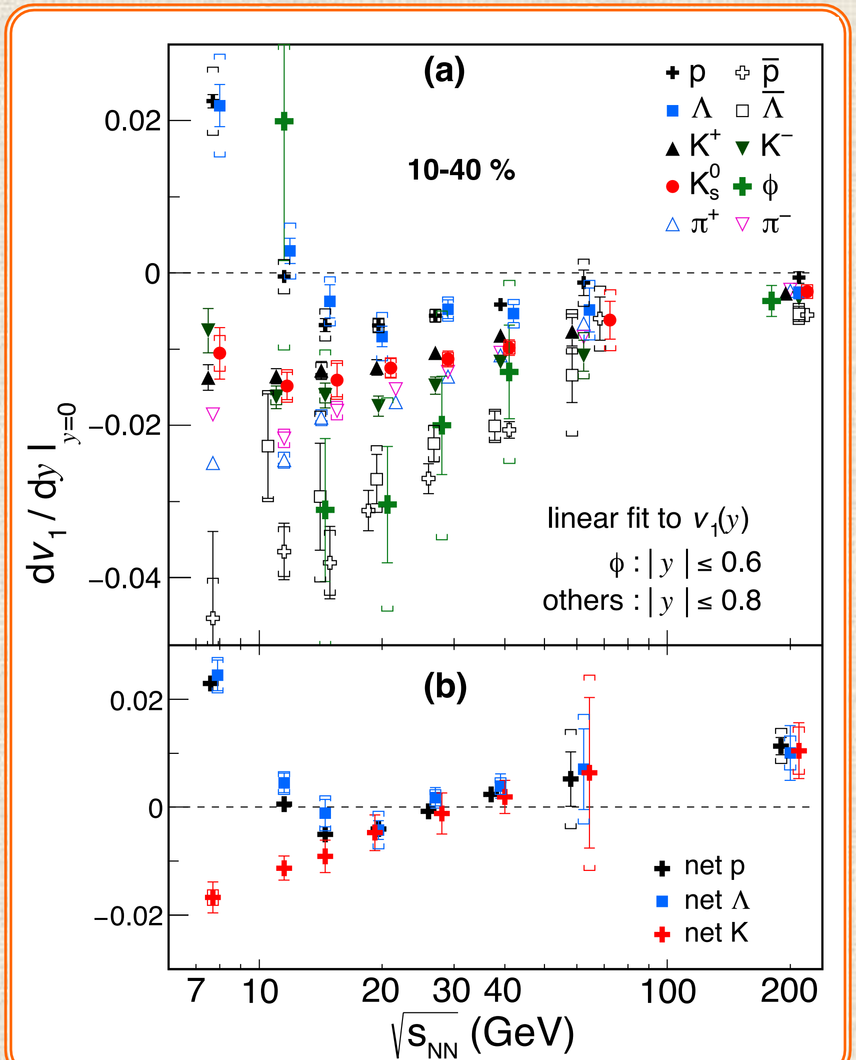

- ★ Proton and Λ v_1 slope: agree within errors and change sign near 11. 5 GeV
- ★ Pion, anti-proton, anti-lambda, $K^{\pm}$ and K_s^0 v_1 slope: always negative. $K^+ > K^-$.
- ★ Net-proton and net-Λ v_1 slope: shows double sign change.

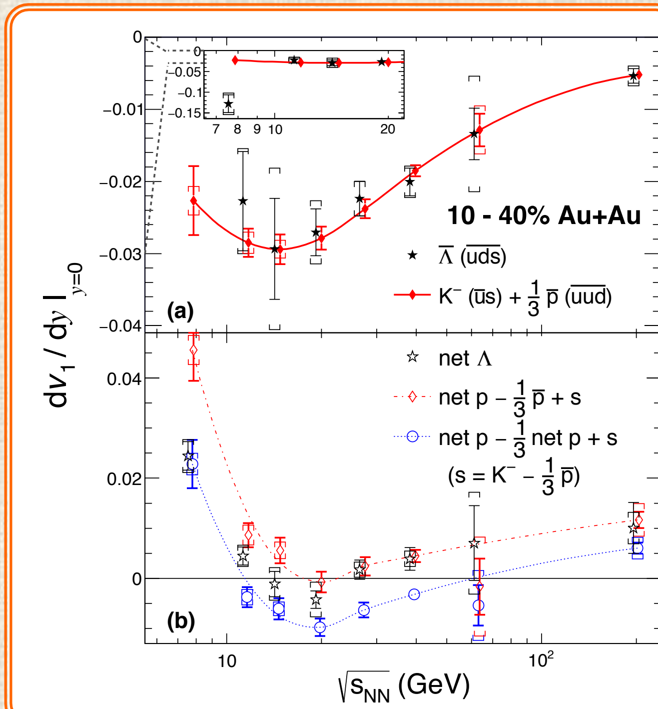

STAR: **arXiv:1708.07132, PRL (accepted)**

★ Consistent with hadron coalescence of constituent quarks

Energy Dependence of v_3

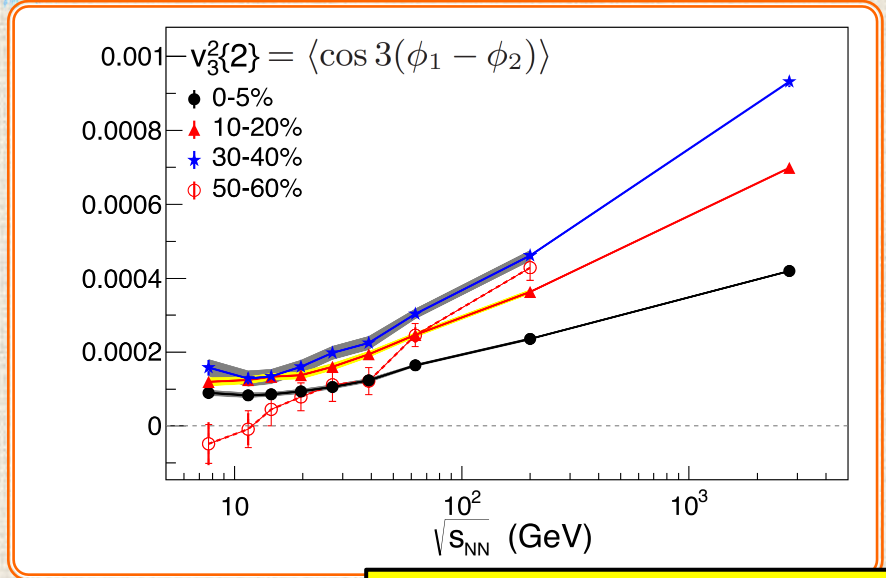

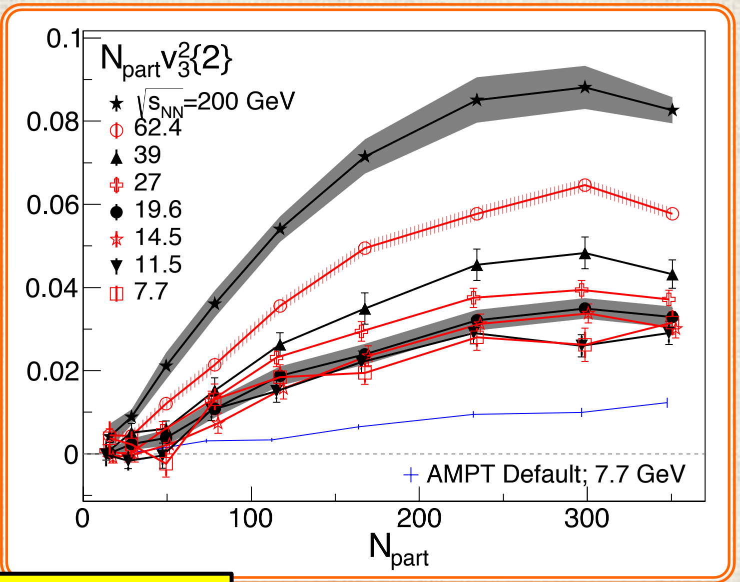

STAR: **Phys.Rev.Lett. 116 (2016) no.11, 112302**

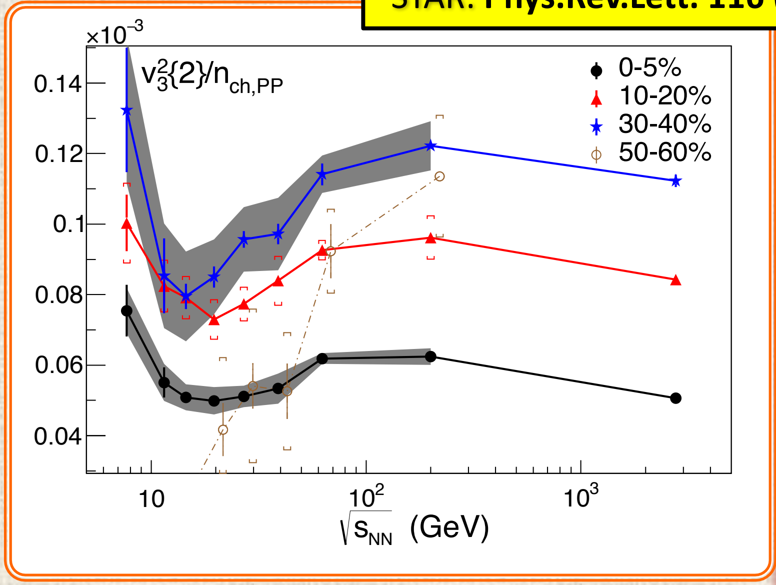

- $v_3^2\{2\}$ - directly related to conversion of **initial density anisotropies** in the overlap region into momentum space correlations through subsequent interactions in the expansion (as revealed via large-$\Delta\eta$ narrow-$\Delta\varphi$ **ridge correlations**).
- In hydro $v_3^2\{2\}$ is sensitive to **low viscosity state** of QGP. (Reduction in the pressure expected during a mixed phase should lead to a reduction in the observed correlations.)

★ **For centralities below 40% down to 7.7 GeV $v_3^2\{2\} \neq 0$. In disagreement with non-QGP models. May the QGP be created even in these low energy collisions !?**

★ **$v_3^2\{2\}/n_{ch,PP}$ shows a minimum near $\sqrt{s_{NN}}$=20 GeV.**

Rapidity correlations of $\pi^{\pm}$ in (0-5)% Au-Au

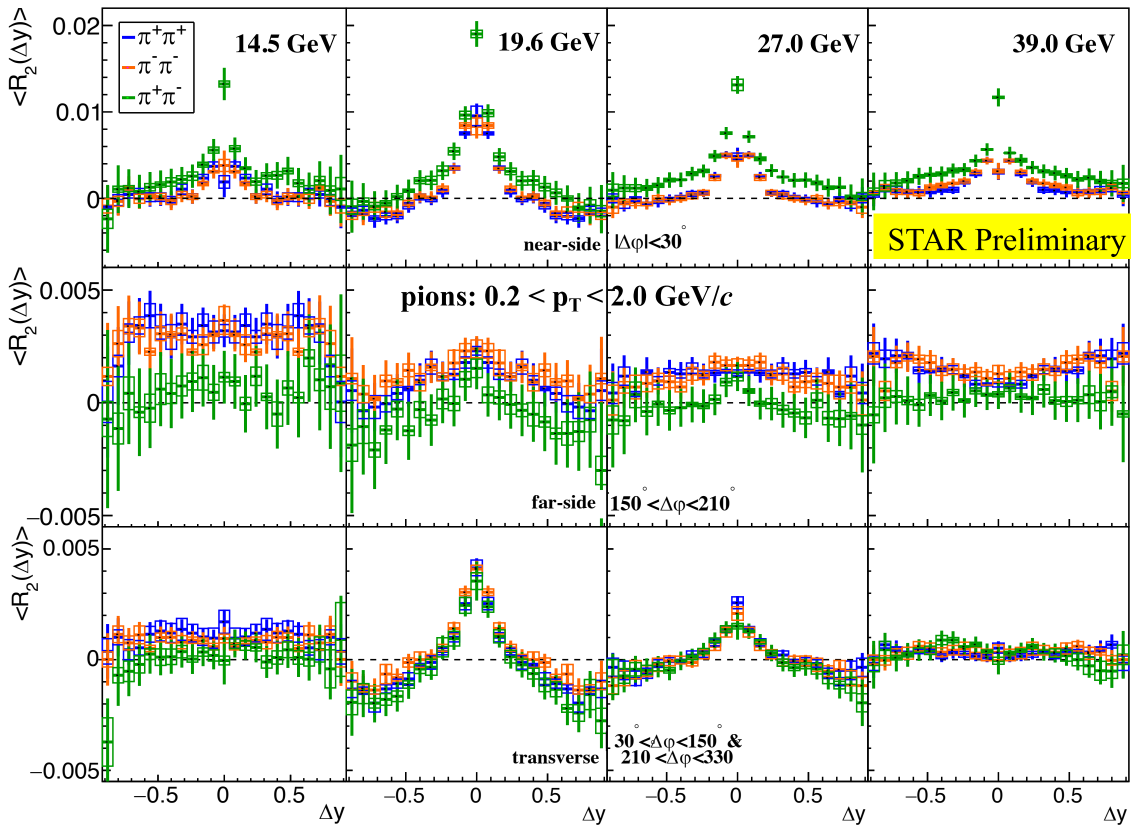

$$R_2(y_1, y_2) = \frac{\langle \rho_2(y_1, y_2) \rangle}{\langle \rho_1(y_1) \rangle \langle \rho_1(y_2) \rangle} - 1$$

- ★ Near-side $|\Delta\phi| < 30^o$ peak around $y \approx 0$ observed for all energies is stronger in $\pi^+\pi^-$ than in $\pi^\pm\pi^\pm$. Results from the short-range correlation mechanisms dominant in this $\Delta\phi$ range.
- ★ No significant structure seen in $150^o < \Delta\phi < 210^o$ (far-side) projection.
- ★ Charge-independent and **beam-energy localized** (19.6 and 27 GeV) structure observed in $R_2(\Delta y)$ extending as a ridge in $30^o < \Delta\phi < 150^o$ & $210^o < \Delta\phi < 330^o$!!!
- ★ The UrQMD ($0^o \le \Delta\phi \le 360^o$) does not reproduce the effect neither for $\pi^+\pi^+$ nor for pp.

arXiv:1708.03364

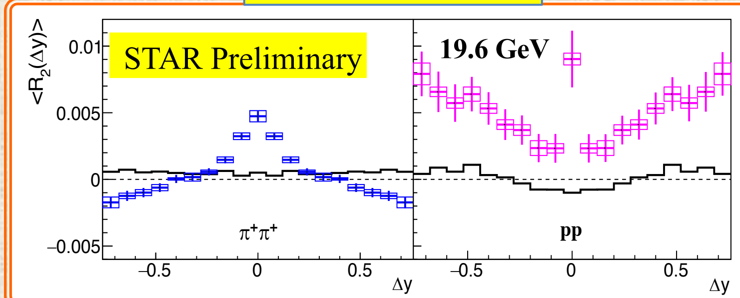

2. Search for the signals of phase boundary: Bulk properties of matter at freeze-out

Bulk Properties at Freeze-out

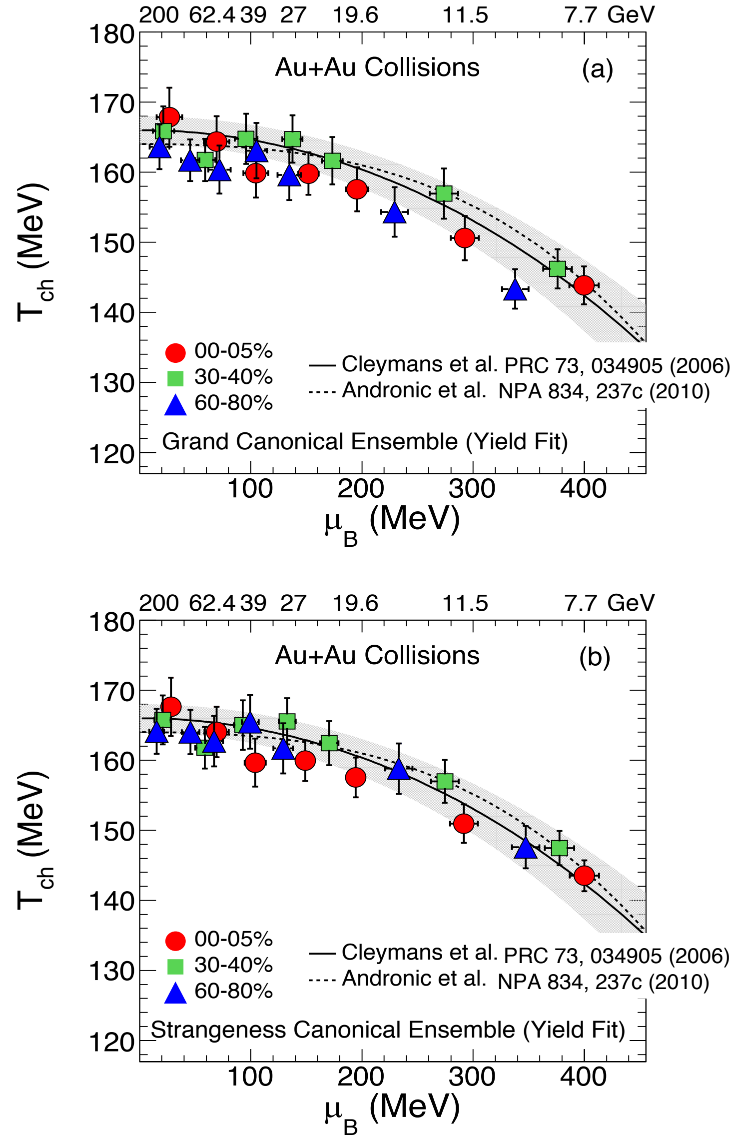

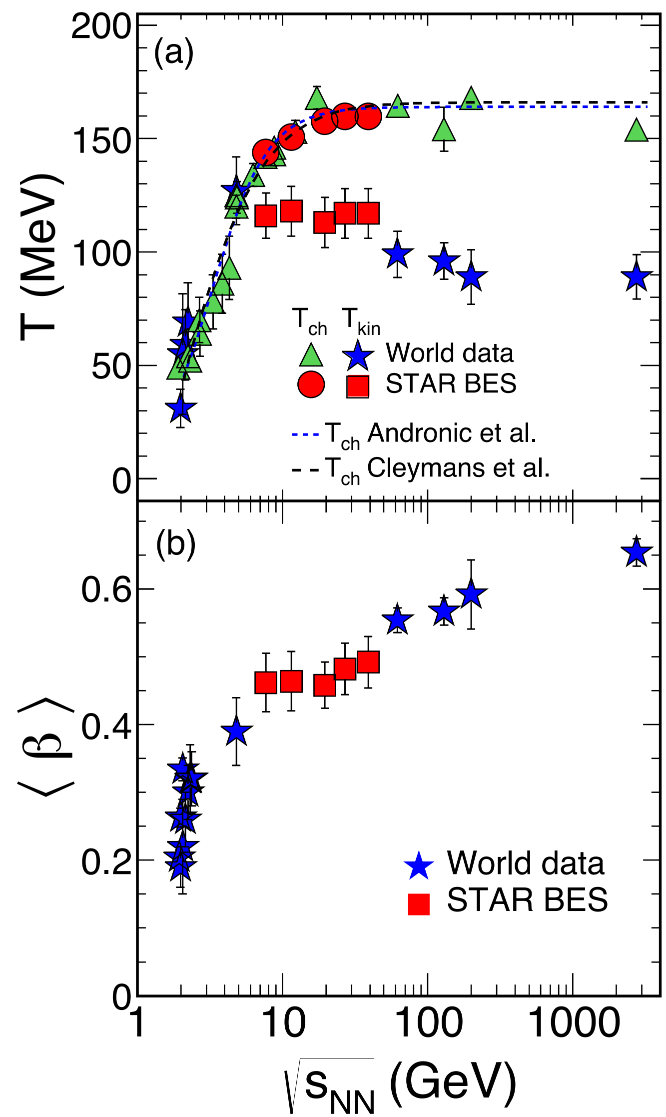

STAR: Phys.Rev. C **96** (2017) 044904

Bulk Properties at Freeze-out

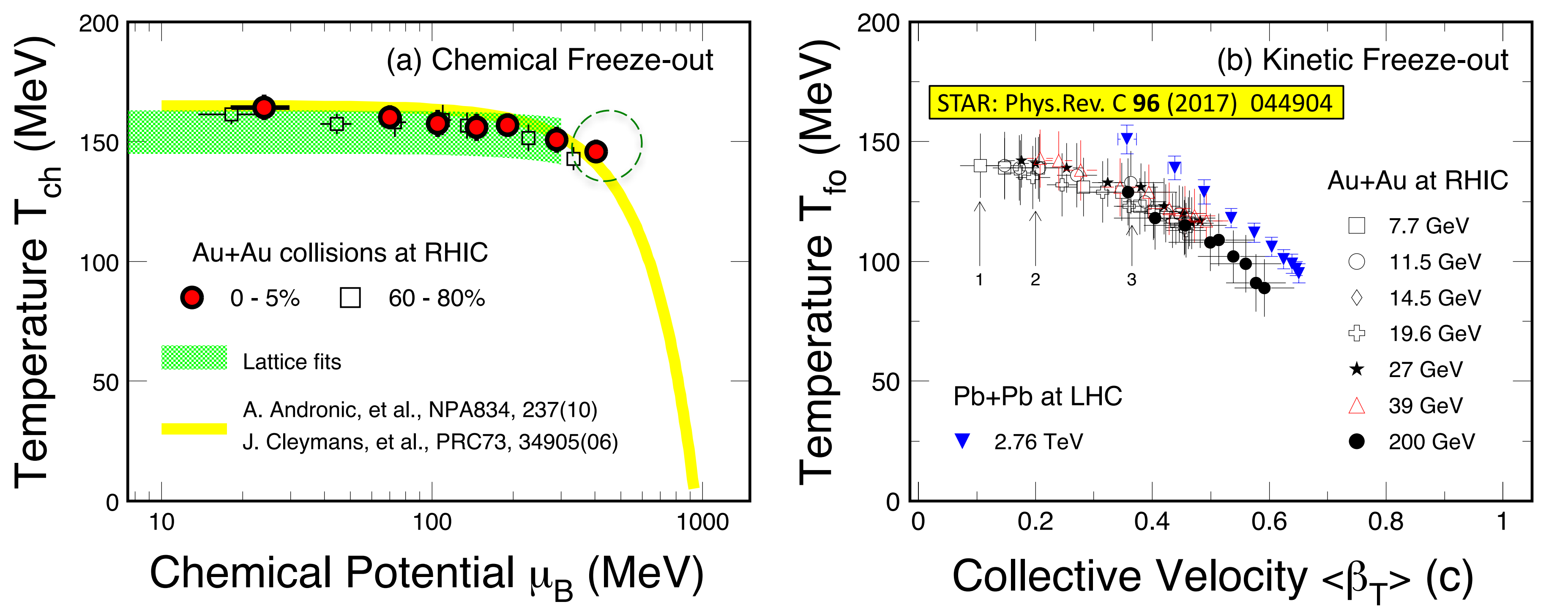

Chemical Freeze-out: (GCE)

- Weak temperature dependence
- Centrality dependence μ_B!
- LGT calculations indicate the Critical Region around **μ_B ~ 300 MeV?**

Kinetic Freeze-out:

- Central collisions => lower value of **T_{fo}** and larger collectivity **β_T**
- **Stronger collectivity at higher energy, even for peripheral collisions**

- ALICE: B.Abelev et al., PRL**109**, 252301(12); Phys.Rev. C**88**, 044910(2013).
- STAR: J. Adams, et al., NPA**757**, 102(05); **STAR**: Phys.Rev. C**96** (2017) 044904
- S. Mukherjee: Private communications. August, 2012

K/π Ratios and Baryon Density

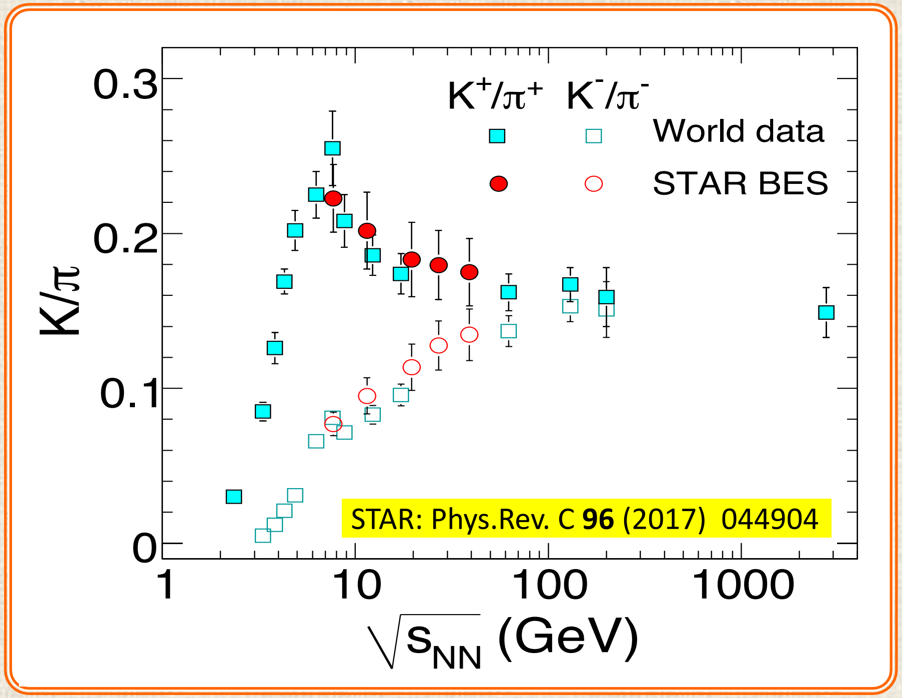

1) The K^+/π ratio peaks at $\sqrt{s_{NN}}$ ~ 8 GeV,
   K^-/π ratio merges with K^+/π at higher collision energy

K/π Ratios and Baryon Density

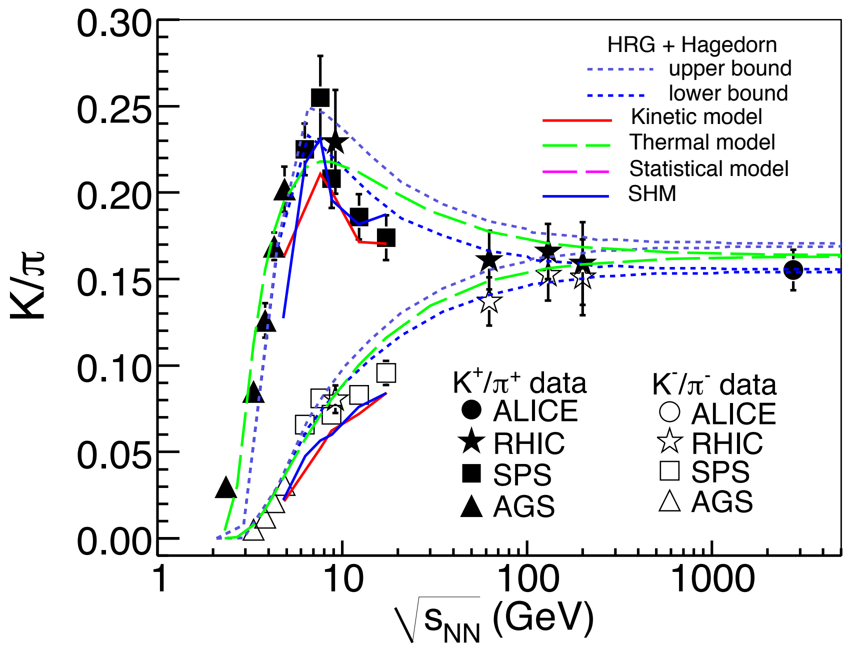

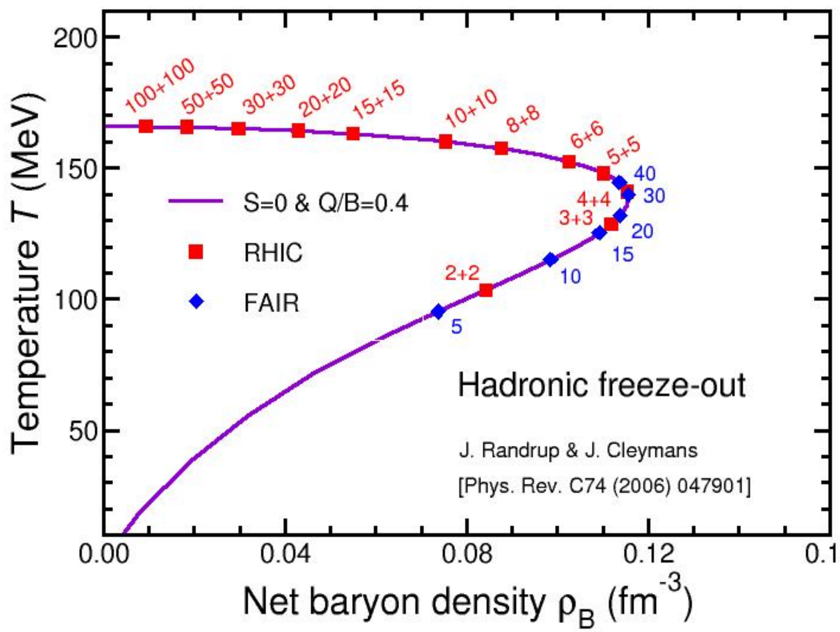

1) The K^+/π ratio peaks at $\sqrt{s_{NN}}$ ~ 8 GeV,
   K^-/π ratio merges with K^+/π at higher collision energy
2) Model: **Net baryon density peaks at $\sqrt{s_{NN}}$ ~ 8 GeV**
3) At **$\sqrt{s_{NN}}$ > 8 GeV, pair production becomes important**

3. Search for the QCD critical endpoint: Fluctuations of conserved quantitities and

Expectation from Model Calculations

$$\frac{p}{T^4} = \frac{1}{VT^3}\ln Z(T,\mu_u,\mu_d,\mu_s) = \sum_{ijk}\frac{1}{i!j!k!}\chi^{uds}_{ijk}\left(\frac{\mu_u}{T}\right)^i\left(\frac{\mu_d}{T}\right)^i\left(\frac{\mu_s}{T}\right)^j$$

$$\chi_2^X = \frac{1}{VT^3}\langle N_X^2\rangle, \qquad \chi_4^X = \frac{1}{VT^3}\left(\langle N_X^4\rangle - 3\langle N_X^2\rangle^2\right)$$

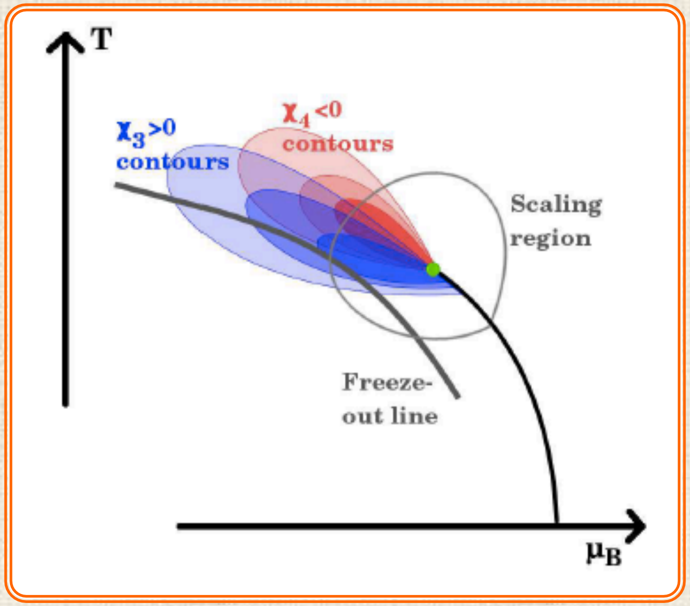

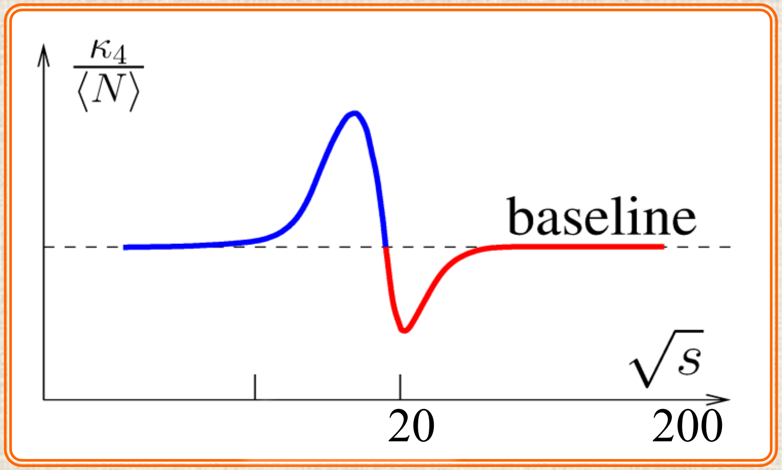

- Characteristic "Oscillating pattern" is expected for the QCD critical point but *the exact shape depends on the location of freeze-out with respect to the location of CEP*
- M. Stephanov, ***PRL107***, 052301(2011)
  - V. Skokov, Quark Matter 2012
  - J.W. Chen, J. Deng, H. Kohyyama, arXiv: 1603.05198, Phys. Rev. **D93** (2016) 034037

N.B. For $\mu_Q = \mu_S = 0$ the leading-order correction to the pressure at non-vanishing μ_B is proportional to the quadratic fluctuations of the net baryon number:

$$\frac{p(T,\mu_B)-p(T,0)}{T^4} = \frac{1}{2}\chi_2^B(T)\left(\frac{\mu_B}{T}\right)^2\left[1+\frac{1}{12}\frac{\chi_4^B(T)}{\chi_2^B(T)}\left(\frac{\mu_B}{T}\right)^2\right] + \mathcal{O}(\mu_B^6)$$

Net-K and net-p distributions

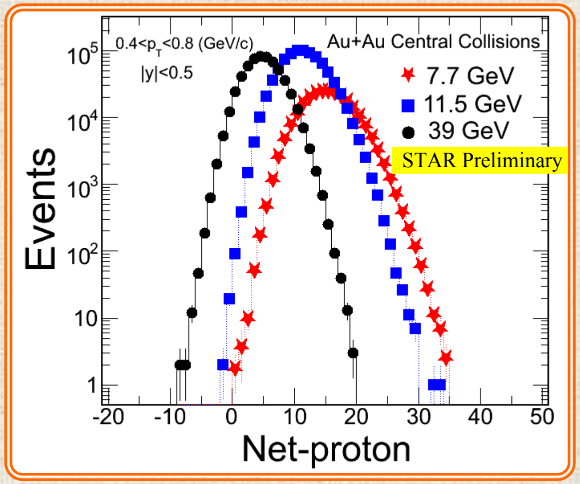

STAR: arXiv:1709.00713

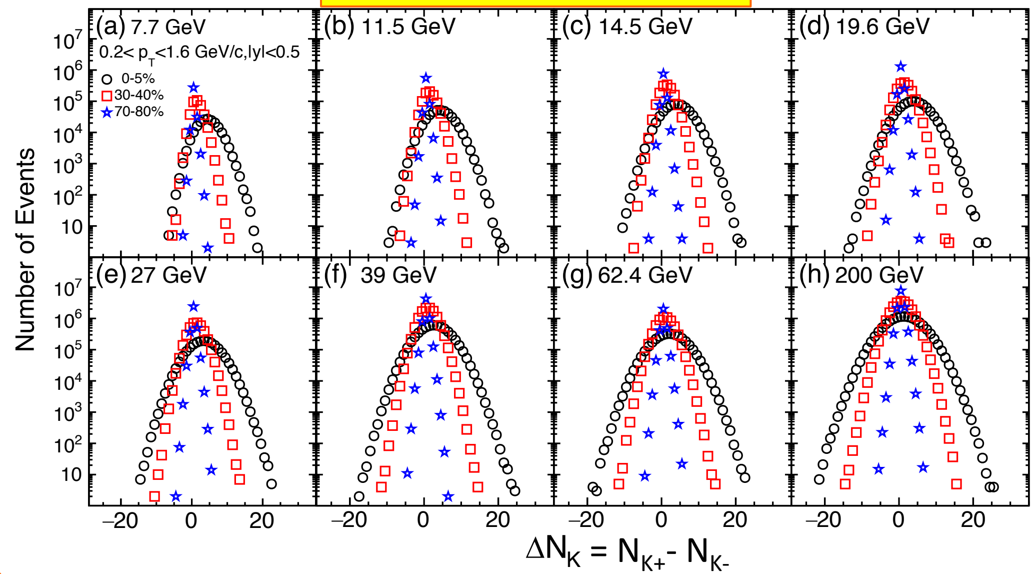

N = net-proton or ΔN_K

From P(N) to cumulants

$\delta N = N - \langle N \rangle$

$C_1 = \langle N \rangle$

$C_2 = \langle (\delta N)^2 \rangle$

$C_3 = \langle (\delta N)^3 \rangle$

$C_4 = \langle (\delta N)^4 \rangle - 3\langle (\delta N)^2 \rangle^2$

Mean (M), variance (σ), skewness S and kurtoisis (κ)

$M = C_1$, $\sigma^2 = C_2$, $S = C_3/(C_2)^{3/2}$, $\kappa = C_4/(C_2)^2$

From cumulants to multi-particle correlators

$$\hat{\kappa}_1 = C_1$$
$$\hat{\kappa}_2 = C_2 - C_1$$
$$\hat{\kappa}_3 = C_3 - 3C_2 + 2C_1$$
$$\hat{\kappa}_4 = C_4 - 6C_3 + 11C_2 - 6C_1$$

Higher Moments of Net-Q, -K, -p

STAR: PRL. 113 (2014) 092301

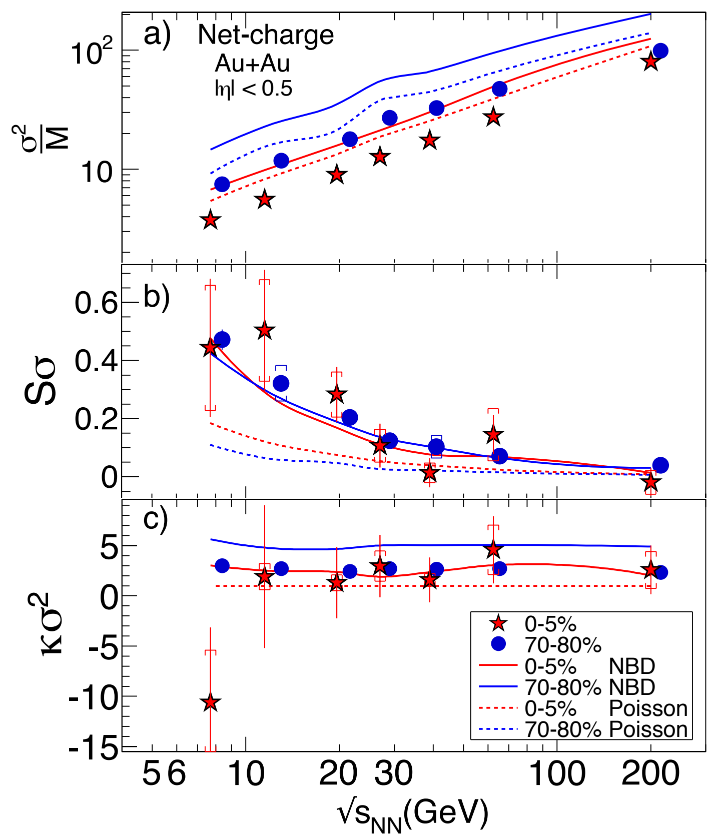

$$\sigma^2/M = C_2/C_1$$
$$M/\sigma^2 = C_1/C_2$$
$$S\sigma = C_3/C_2$$
$$\kappa\sigma^2 = C_4/C_2$$

STAR: arXiv:1709.00713

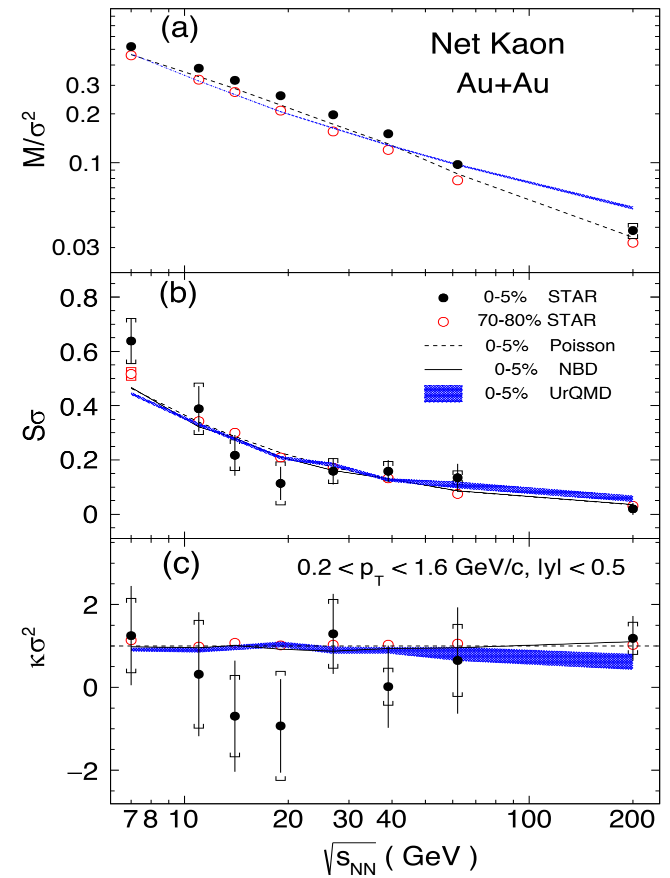

☹ The net-Q shows flat energy dependence.

☹ The net-Kaon shows flat energy dependence.

Higher Moments of Net-Q, -K, -p

STAR: arXiv:1709.00713

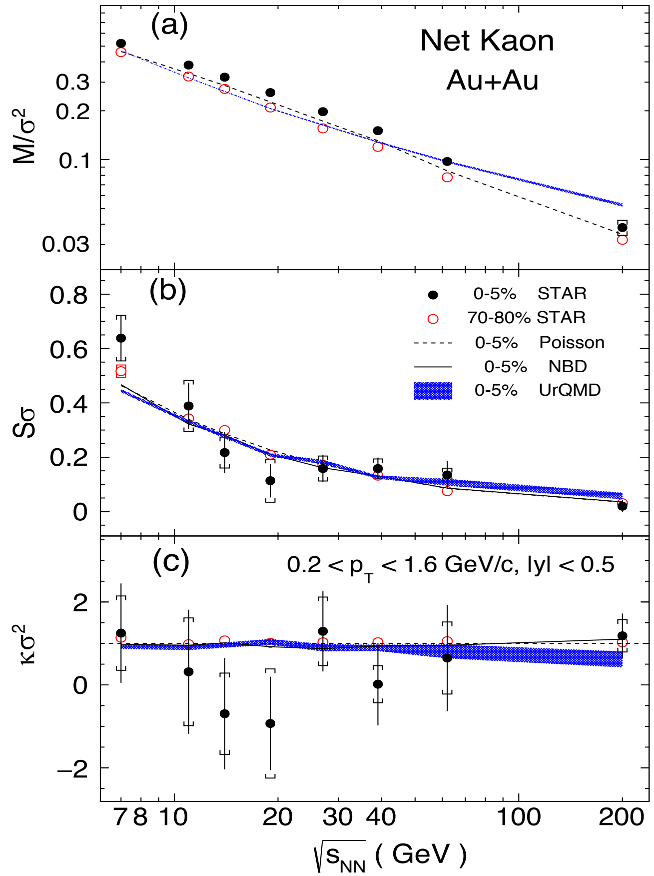

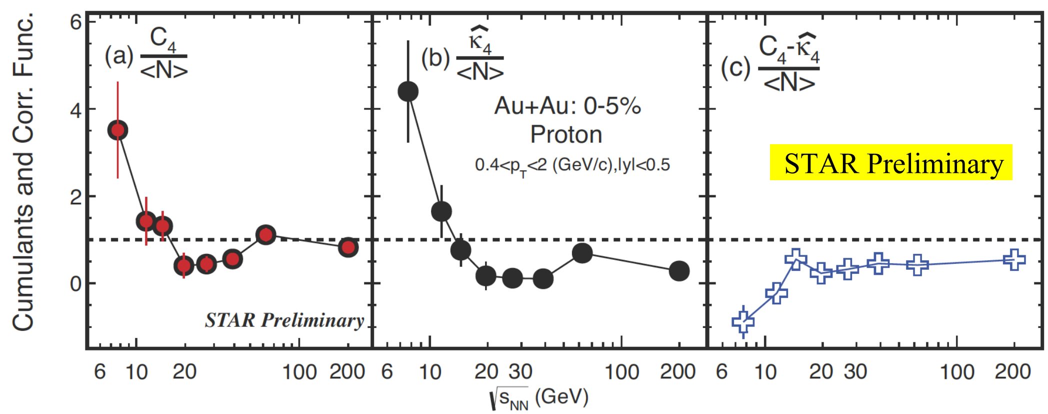

$M/\sigma^2 = C_1/C_2$
$S\sigma = C_3/C_2$
$\kappa\sigma^2 = C_4/C_2$

☹ The net-Kaon shows flat energy dependence.

★ Net-p shows **non-monotonic energy dependence** in the most central Au+Au collisions starting at **$\sqrt{s_{NN}}$** < 27 GeV!

Beam Energy Scan Phase- II

2019-2020: BES-II at RHIC

$\sqrt{s_{NN}}$ (GeV)	Events (10^6)	BES-II / BES-I	Weeks	μ_B (MeV)	T_{CH} (MeV)
200	350	2010		25	166
62.4	67	2010		73	165
54.4	**1200**	**2017**			
39	39	2010		112	164
27	70	2011		156	162
19.6	**400** / 36	**2019-20** / 2011	**3**	206	160
14.5	**300** / 20	**2019-20** / 2014	**2.5**	264	156
11.5	**230** / 12	**2019-20** / 2010	**5**	315	152
9.1	**160** / 0.3	**2019-20** / 2008	**9.5**	355	140
7.7	**100** / 4	**2019-20** / 2010	**14**	420	140

Precision measurements,
map the QCD phase diagram **$200 < \mu_B < 420$MeV**

CBM Phase-0 Exp: eTOF@STAR

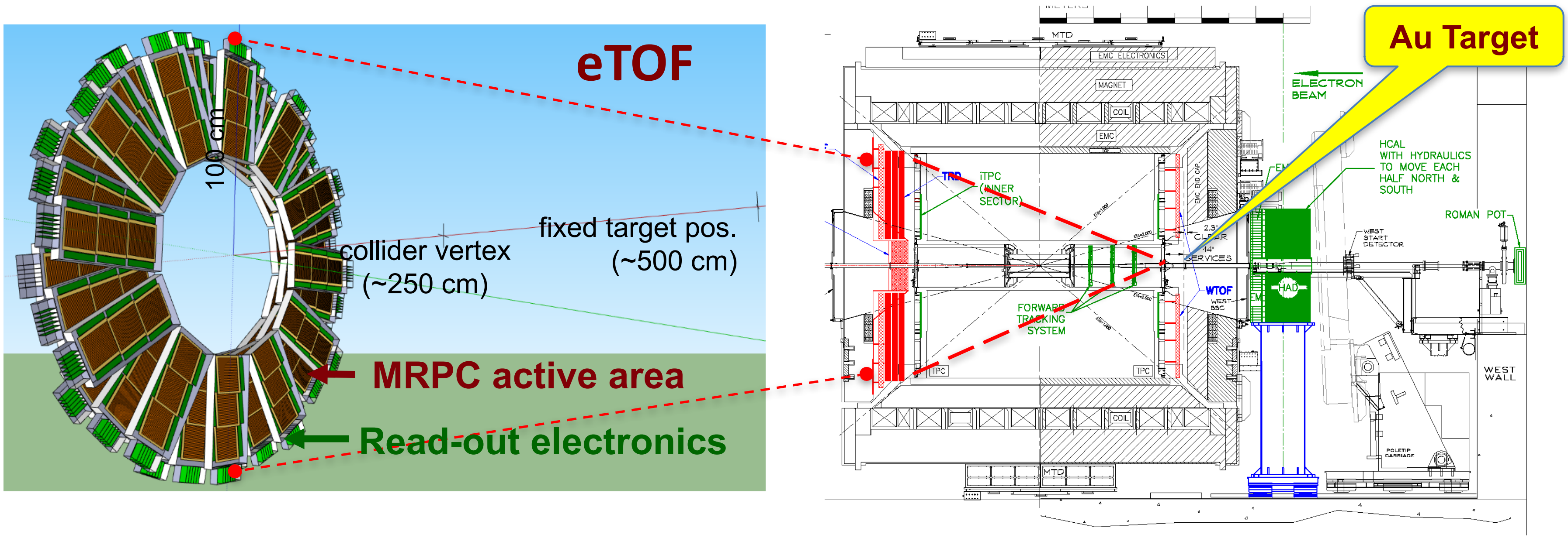

Install, commission and use 10% of the CBM TOF modules, including the read-out chains at STAR, starting in 2019

CBM participating in RHIC Beam Energy BES-II in 2019-2020:

- Complementary to part of CBM's physics program:
  $\sqrt{s_{NN}}$ = **3**, **3.5**, **3.9**, **4,5**, 7.7 GeV (**750 ≤ μ_B ≤ 420 MeV**)
  especially for ***B-*** & ***s-hadrons*** production and fluctuations

LHC+RHIC
QGP properties
$\mu_B \approx 0$
now - **2026**

RHIC BES-II
collider mode
$200 < \mu_B < 420$ MeV
2019 & 2020

Fixed-target
BES-III
$350 < \mu_B < 750$ MeV
2019 – **CBM**

Adapted from Nu Xu

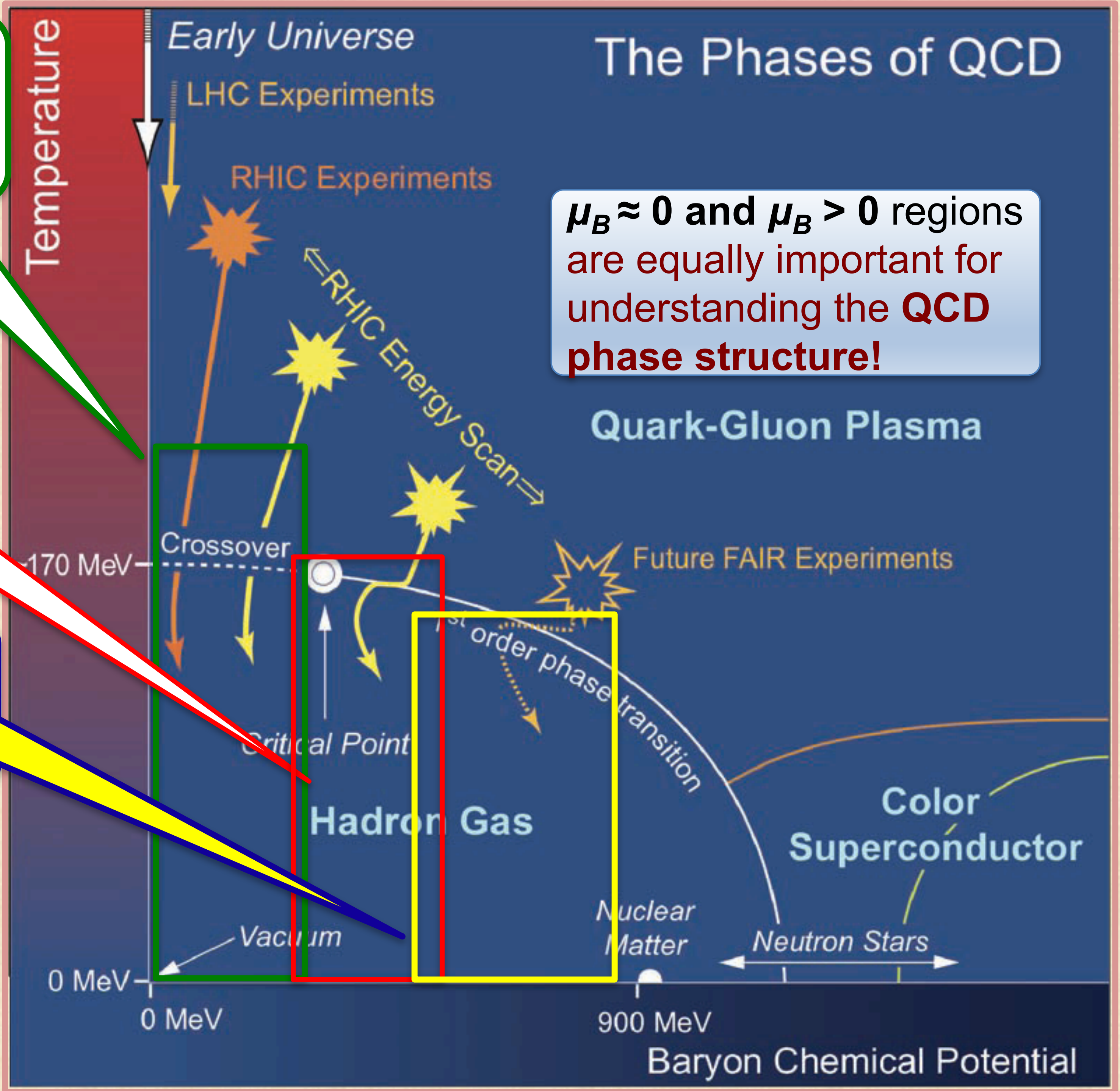

M. Šumbera

Summary

- **STAR results from BES program covering large μ_B range provide important constraint on the QCD phase diagram:**
  - High-p_T suppression and its further evolution into enhancement at lower $\sqrt{s_{NN}}$ is driven by mesons. Baryons up to $\sqrt{s_{NN}}$=62.4 GeV remain enhanced.
  - No significant energy dependence of the J/ψ suppression from SPS to RHIC was found.
  - Integrated excess yield of LMR di-electrons normalized by dN_{ch}/dy, is proportional to lifetime of fireball from $\sqrt{s_{NN}}$ = 17.3 GeV to $\sqrt{s_{NN}}$ = 200 GeV.
  - Directed flow slopes of net-proton and net-Λ $dv_1/dy|_{y=0}$ show double sign change.
  - For centralities < 40% down to $\sqrt{s_{NN}}$=7.7 GeV $v_3^2\{2\} \neq 0$. In disagreement with non-QGP models. $v_3^2\{2\}/n_{ch,PP}$ shows a minimum near $\sqrt{s_{NN}}$=20 GeV.
  - Charge-independent and beam-energy localized (19.6 and 27 GeV) structure observed in $R_2(\Delta y)$ extending as a ridge in $30^o < \Delta\phi < 150^o$ & $210^o < \Delta\phi < 330^o$
  - K^+/π ratio peaks at $\sqrt{s_{NN}}$ ~ 8 GeV, i.e. @ maximal net-baryon density.
  - Net-p shows non-monotonic energy dependence in the most central collisions starting at $\sqrt{s_{NN}}$ < 27 GeV.

- **Search for the critical endpoint continues:**
  - BES-II program is scheduled for 2019-20.
  - Fixed target program executed jointly with the CBM is scheduled for 2019. It will extend the measurements up to $\mu_B \approx 750$ MeV.

STAR Collaboration

Thank You

Argonne National Laboratory, Argonne, Illinois 60439
Brookhaven National Laboratory, Upton, New York 11973
University of California, Berkeley, California 94720
University of California, Davis, California 95616
University of California, Los Angeles, California 90095
Universidade Estadual de Campinas, Sao Paulo, Brazil
University of Illinois at Chicago, Chicago, Illinois 60607
Creighton University, Omaha, Nebraska 68178
Czech Technical University in Prague, FNSPE, Prague, 115 19, Czech Republic
Nuclear Physics Institute AS CR, 250 68 Řež/Prague, Czech Republic
University of Frankfurt, Frankfurt, Germany
Institute of Physics, Bhubaneswar 751005, India
Indian Institute of Technology, Mumbai, India
Indiana University, Bloomington, Indiana 47408
Alikhanov Institute for Theoretical and Experimental Physics, Moscow, Russia
University of Jammu, Jammu 180001, India
Joint Institute for Nuclear Research, Dubna, 141980, Russia
Kent State University, Kent, Ohio 44242
University of Kentucky, Lexington, Kentucky, 40506-0055
Institute of Modern Physics, Lanzhou, China
Lawrence Berkeley National Laboratory, Berkeley, California 94720
Massachusetts Institute of Technology, Cambridge, MA
Max-Planck-Institut f"ur Physik, Munich, Germany
Michigan State University, East Lansing, Michigan 48824
Moscow Engineering Physics Institute, Moscow Russia

NIKHEF and Utrecht University, Amsterdam, The Netherlands
Ohio State University, Columbus, Ohio 43210
Old Dominion University, Norfolk, VA, 23529
Panjab University, Chandigarh 160014, India
Pennsylvania State University, University Park, Pennsylvania 16802
Institute of High Energy Physics, Protvino, Russia
Purdue University, West Lafayette, Indiana 47907
Pusan National University, Pusan, Republic of Korea
University of Rajasthan, Jaipur 302004, India
Rice University, Houston, Texas 77251
Universidade de Sao Paulo, Sao Paulo, Brazil
University of Science \& Technology of China, Hefei 230026, China
Shandong University, Jinan, Shandong 250100, China
Shanghai Institute of Applied Physics, Shanghai 201800, China
SUBATECH, Nantes, France
Texas A&M University, College Station, Texas 77843
University of Texas, Austin, Texas 78712
University of Houston, Houston, TX, 77204
Tsinghua University, Beijing 100084, China
United States Naval Academy, Annapolis, MD 21402
Valparaiso University, Valparaiso, Indiana 46383
Variable Energy Cyclotron Centre, Kolkata 700064, India
Warsaw University of Technology, Warsaw, Poland
University of Washington, Seattle, Washington 98195
Wayne State University, Detroit, Michigan 48201
Institute of Particle Physics, CCNU (HZNU), Wuhan 430079, China
Yale University, New Haven, Connecticut 06520
University of Zagreb, Zagreb, HR-10002, Croatia

Backup slides

Elliptic flow of identified (anti)particles

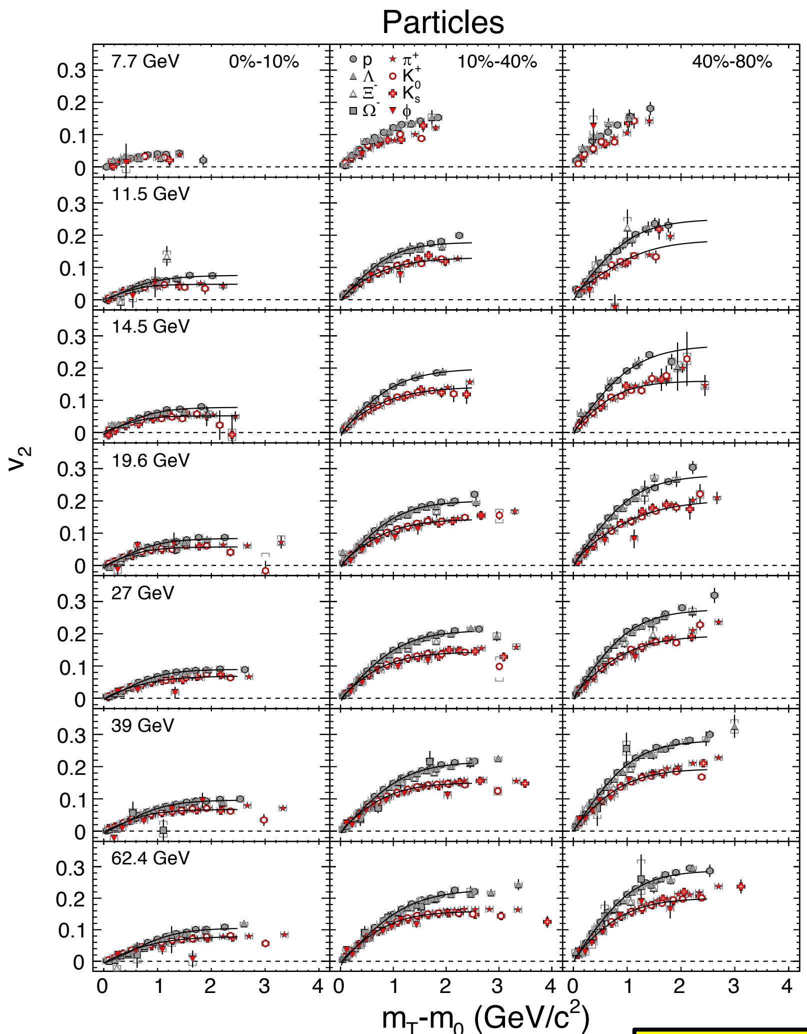

$\sqrt{s_{NN}}$

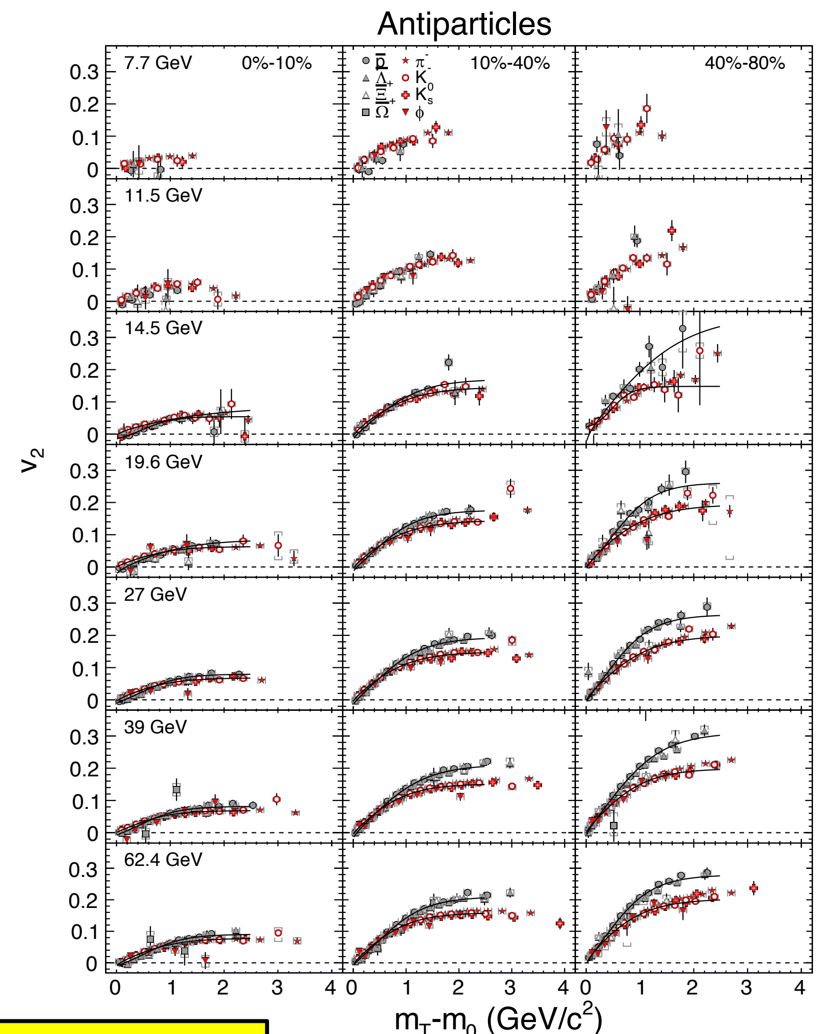

STAR: **Phys.Rev. C93, 014907 (2016)**

Starting from 14.5 GeV similar relative v_2 baryon-meson splitting is observed for all centralities (and agrees within 15% with the NCQ quark scaling – see line fits).
The larger v_2 for most particles relative to antiparticles shows a clear centrality dependence.

Status on Predictions

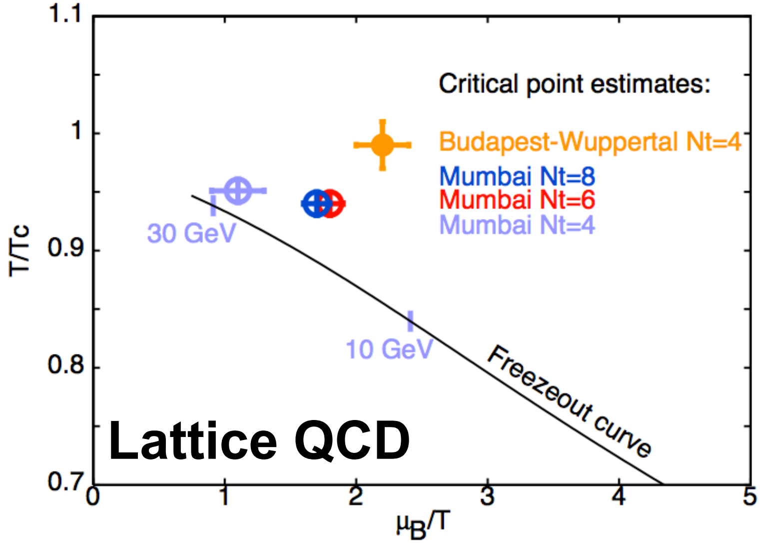

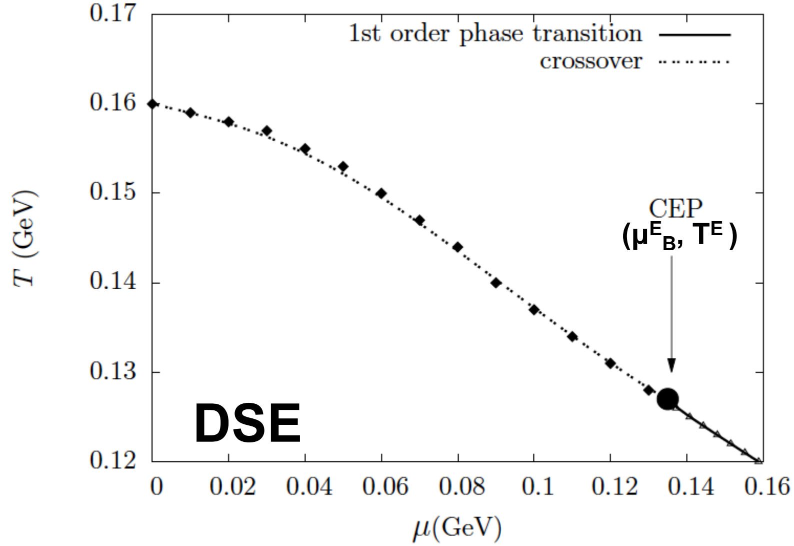

Lattice QCD:

1) Fodor and Katz, JHEP 0404,050 (04)
   (μ^E_B, T_E)= (360, 162) MeV (Re.)
2) Gavai and Gupta, NPA 904, 883c (13)
   (μ^E_B, T_E)= (279, 155) MeV (Taylor)
3) F. Karsch (μ^E_B/T_E >2, CPOD2016)

Dyson-Schwinger Equation:

1) Y. X. Liu, et al., PRD90, 076006(14)
   (μ^E_B, T^E) = (372, 129) MeV
2) H.S. Zong et al., JHEP 07, 014(14)
   (μ^E_B, T_E)= (405, 127) MeV
3) C.S. Fischer et al., PRD90, 034022(14)
   (μ^E_B, T^E) = (504, 115) MeV

μ^E_B =300 ~ 504 MeV, T_E =115~162 MeV, **$\mu^E_B/T_E > 2.5$**